Field Validation of Wisconsin Modified Binder Selection Guidelines

Wisconsin Highway Research Project: 0092-03-13

by

Rodrigo Delgadillo, Research Assistant
Arash Motamed, Research Assistant
Hussain Bahia, Professor
University of Wisconsin – Madison
Department of Civil and Environmental Engineering
1415 Engineering Drive, Madison, WI 53706-7910

October 2007

DISCLAIMER

This research was funded through the Wisconsin Highway Research Program by the Wisconsin Department of Transportation and the Federal Highway Administration under Project # (0092-03-13). The contents of this report reflect the views of the authors who are responsible for the facts and the accuracy of the data presented herein. The contents do not necessarily reflect the official views of the Wisconsin Department of Transportation or the Federal Highway Administration at the time of publication.

This document is disseminated under the sponsorship of the Department of Transportation in the interest of information exchange. The United States Government assumes no liability for its contents or use thereof. This report does not constitute a standard, specification, or regulation.

The United States Government does not endorse products or manufacturers. Trade and manufacturers' names appear in this report only because they are considered essential to the object of the document.

TECHNICAL REPORT DOCUMENTATION PAGE

1. Report No.: WHRP	2. Government Accession No.:	3. Recipient's Catalog No.:
4. Title and Subtitle Field Validation of Wisconsin Modified Binder Selection Guidelines		5. Report Date: June 2007 6. Performing Organization Code: 0092-03-13
5. Authors: Rodrigo Delgadillo (Research Assistant), Arash Motamed 6. (Research Assistant) and Hussain Bahia (Professor)		Performing Organization Report No. : 0092-03-13
9. Performing Organization Name and Address University of Wisconsin – Madison Department of Civil and Environmental Engineering 1415 Engineering Drive, Madison, WI 53706-2507		10. Work Unit No. (TRAIS) 11. Contract or Grant No. WisDOT SPR# 0092-03-13
12. Sponsoring Agency Name and Address Wisconsin Department of Tranportation Division of Transportation Infrastructure Development Research Coordination Section 4802 Sheboygan Ave. Box 7065, Madison, WI 53707 – 7910		13. Type of Report and Period Covered Final Report: 2003 - 2007 14. Sponsoring Agency Code
15. Supplementary Notes		

16. Abstract

In June 2005, a report with Modified Binder Selection Guidelines for Wisconsin was finished under the sponsorship of the Wisconsin Highway Research Program. The report name is Development of Guidelines for PG Binder Selection in Wisconsin (SPR# 0092-01-01). In that report five areas were covered for the guidelines: binder storage and stability; mixing and compaction temperatures of binders; fatigue characterization; low temperature cracking and rutting characterization. The results of the project included the development of new specification guidelines. The new specifications included some new parameters: Zero Shear Viscosity ZSV mixing and compaction temperatures limits; a critical cracking temperature obtained using BBR, DTT and Tg testing for low temperature characterization; a fatigue parameter called Np20 obtained by time sweep testing in the DSR; and a rutting parameter called Gv obtained by repeated creep and recovery using the DSR. The present report deals with the field validation of these new parameters. It is divided in four chapters. Each one dealing with one of the topics. The first chapter is Mixing and Compaction Temperatures. Eight different projects were surveyed and sampled for this section. The study concluded that compaction in the field happens at temperatures ranging from 120ºC to 70ºC. The compaction temperatures from ZSV are too high and no realistic. The temperature at which the binder has a low shear viscosity of 50 Pa·s is recommended as a lower limit for compaction in the field. The mixing temperatures using ZSV are lower and more appropriate than the ones recommended by the Superpave Criteria. The current procedure for determining ZSV temperatures, however, includes significant extrapolations that make the results inaccurate. A better procedure should be developed before implementing this method.

Eight projects were considered for the fatigue validation. The fatigue parameter Np20 showed good correlation with the longitudinal cracking in the field. No good correlation was found between $G^*\sin\delta$ and the field data. A new surrogate test using stress sweep was also compared with field data and no good correlation was found.

The results of the low temperature study indicated that the current Superpave criteria of S(60) = 300 MPa, from BBR data, shows good correlation with field transverse cracking. I seems that there is no need to use the DTT or Tg for low temperature characterization.

No conclusive results could be obtained from the rutting study. None of the six projects followed for this section showed any rutting during the duration of this study. The research team, however, maintains the validity of the new parameter Gv. The prediction of allowable ESALs for each project, based on Gv, are higher than the the accumulated traffic until now. This agrees with the field performance that shows no rutting damage up to date.

17. Key Words	18. Distribution Statement No restriction. This document is available to the public through the National Technical Information Service 5285 Port Royal Road, Springfield VA 22161		
19. Security Classif.(of this report) Unclassified	19. Security Classif. (of this page) Unclassified	20. No. of Pages	21. Price

AKNOWLEDGEMENTS

This study was sponsored by the Wisconsin Highway Research Program. The continuous support of the WisDOT is greatly appreciated. Specials thanks to Judie Ryan, Thomas Brokaw, Nancy Bushe, Richard Barden, Michael Malaney and Laura Finley, from the WisDOT. The help of Andrew Hanz from the WHRP is also acknowledged and appreciated.

The authors gratefully acknowledge the cooperation of the Paine & Dolan and Mathy Construction staff in facilitating access to projects and collection of samples. The following UW students contributed in the laboratory testing: Aaron Bonk, Adekunle Mofolasayo, Joshua Ojo and Ashley Reinke, their help is greatly appreciated.

EXECUTIVE SUMMARY

Overview

The present project consisted of the field validation of selection guidelines for modified asphalt binders. These guidelines were developed previously (WHRP SPR#0092-01-01). The project has four main focus areas: mixing and compaction temperatures, fatigue performance, rutting performance and low temperature cracking. Validation for the guidelines in those four areas was sought during this project. The methodology for the validation consisted of comparing laboratory data obtained using the procedures suggested in SPR#0092-01-01 with the field pavement performance for the selected projects. A database was developed for allowing future updates on the pavement performance that could be used to improve the field validations.

Background

In the United States, a number of State Highway Agencies claim that the Superpave specification has some critical gaps, mostly related to the performance characterization of modified binders. Recognizing this fact, AASHTO sponsored project NCHRP 9-10, and in 2001, NCHRP Report 459 was published. The report offered a revised system for testing and evaluation of asphalt binders based on damage behavior. A scheme to conduct binder testing for rutting, fatigue, glass transition temperature, and workability that would allow a more direct qualification of modified binders for specific climate and traffic conditions was presented. In 2005, a research effort sponsored by WHRP addressed the implementation of the system for testing and evaluating asphalt binders in Wisconsin (SPR#0092-01-01). The results of the project included the development of new specification guidelines. The new specifications included some new parameters: Zero Shear Viscosity (ZSV) mixing and compaction temperatures limits; a

critical cracking temperature obtained using BBR, DTT and Tg testing for low temperature characterization; a fatigue parameter called N_{P20} obtained by time sweep testing in the DSR; and a rutting parameter called G_v obtained by repeated creep and recovery using the DSR.

The present report deals with the field validation of these new parameters. It is divided into four chapters: mixing and compaction temperatures, low temperature cracking, fatigue and rutting.

Methodology

The methodology used in this work included the following steps:

- Selection of field sections: Field sections were selected trying to get a wide variety of asphalt binders so the results could have a more general applicability. The majority of sections included PMA asphalt binders.
- Collect samples and conduct testing. Samples were taken for quality control of binders and loose mixtures. The samples were tested and data was entered into a database.
- Monitor performance of sections. The presence and evolution of distresses was monitored for the selected pavements. For the mixing and compaction temperatures, density and temperature data during construction was obtained.
- Develop a database. A database was generated with the field performance and laboratory data. This database could be used in the future to update the performance data.
- Analyze field and laboratory data. By comparing the testing results and the binder guidelines suggested by previous research, conclusions could be made about the validity of those guidelines.

Findings and Recommendations

The main findings of this research are presented as follows for each of the research topics: mixing and compaction temperatures, fatigue cracking, low temperature cracking and rutting damage.

- Mixing and Compaction: It is clear from this study, that compaction temperatures currently used in the field could be reduced without reduction in density. This is observed for modified and unmodified binders. It is recommended that WisDOT, in collaboration with contractors, spend an effort to verify the results of this study and develop guidelines to target the optimum zone construction temperatures. In laboratory mix design procedures, temperatures at which viscosities equal to 50 Pa·s should be used. This will encourage contractors to realize that the high temperatures used today in the field are not necessary.
- Fatigue: Although the parameter proposed in the previous study (Np20) showed good correlation with longitudinal cracking, it is premature to make specific recommendations. The reason being the existing database does not allow differentiating joint cracks and wheel path cracks.
- Thermal Cracking: Field data correlated extremely well with BBR S(60) measurements. There appears to be no need to change the existing practice of the DOT. The limited data collected for DTT can not be used to justify the need for it.
- Rutting: The section that followed during the duration of the project did have not shown any sign of rutting damage yet. MSCR $\%\varepsilon_r$ and $G^*/\sin\delta$ give a fair correlation. With the limited data it is not clear whether we need to change $G^*/\sin\delta$. However, it is clear that

the MSCR test can be used to differentiate between modified and unmodified binders. The issue of replacing $G^*/\sin\delta$ with G_v and MSCR test can not be concluded due to the lack of rutting on the pavement sections.

- Database: An electronic copy of performance and materials database has been developed and delivered for the project. It is highly recommended that the database be maintained and updated for future changes in asphalt grading in Wisconsin.

TABLE OF CONTENTS

LIST OF TABLES

LIST OF FIGURES

CHAPTER ONE: MIXING AND COMPACTION TEMPERATURES

1.1 ZSV And Superpave Mixing And Compaction Temperatures

Between Fall 2003 and Fall 2005, samples were taken from eight asphalt paving projects in Wisconsin. Table 1.1 shows the project and sample information.

TABLE 1.1 Project and Sample Information

Project Name	DOT Project ID*	Layer	Binder	Polymer Modified	Mixture	Date Sampled
STH 17 Rhinelander Bypass	9040-09-70	Base	58 - 34	YES	E-3 19mm	Sep-03
I – 94 Baldwin	1020-01-74	Surface	70 - 28	YES	E-30 12.5mm	Oct-03
STH 95 Arcadia - Fountain City	7132-04-61	Surface	58 - 28	NO	E-1 12.5mm	May-04
STH 95, Arcadia – Fountain City (Intersection)	7132-04-61	Surface	64 - 28	YES	E-1 12.5mm	May-04
USH 51, Iron County	1170-13-70	Surface	64 - 34	YES	E-10 12.5mm	Jun-05
Hanley Rd. Intersection Hudson	7200-05-70	Surface	70 - 28	YES	E-10 19mm	Sep-05
Lindale Dr. Appleton	20050412025 (contract #)	Surface	64 - 28	YES	E-30 12.5mm	Sep-05
Madison Beltline (Midvale-Gammon)	5300-04-74	Surface	64 - 28	YES	E-10 12.5mm	Oct-05

* Refers to the project # assigned by the Wisconsin DOT

To determine the mixing and compaction temperatures, the binder samples were tested using the Brookfield viscometer model DV-II. The Superpave mixing and compaction temperatures were obtained by testing the binders at 20 RPM and using two temperatures: 165ºC and 135ºC. The mixing temperature recommended by Superpave is the one at which the viscosity at 20 RPM is 0.17 Pa·s (±10%). The Superpave compaction temperature is the one that shows a viscosity of 0.28 Pa·s (±10%). After obtaining the viscosities at 165ºC and 135ºC, the mixing and compaction

temperatures were found by interpolating between those values. Some of the mixing temperatures were found to be a above 165ºC. In these cases extrapolation was used, which does not introduce significant errors, since the values were not higher than 170ºC. The only exception to this is binder #7200-05-70, whose Superpave mixing temperature (181ºC) might not be completely accurate. Two samples were tested for each binder to assure repeatability, which was chosen as ± 7ºC (approximate 5%). In case of discrepancy, a third sample was tested and the two closest values were reported. Table 1.2 shows the Superpave mixing and compaction temperatures for the eight binders (average of the two tested samples).

TABLE 1.2 Superpave and ZSV Mixing and Compaction Temperatures

Project ID	Binder	Mixing Temperatures* ºC		Compaction Temperatures* ºC	
		Superpave	ZSV	Superpave	ZSV
9040-09-70	58 - 34	158	153	144	138
1020-01-74	70 - 28	173	164	163	150
7132-04-61	58 - 28	145	136	131	123
7132-04-61 (Inters.)	64 - 28	160	154	148	140
1170-13-70	64 - 34	169	187	158	164
7200-05-70	70 - 28	181	161	170	150
20050412025	64 – 28	170	151	156	138
5300-04-74	64 - 28	167	154	154	138

* Average value. The temperature range is ±10% off this value.

The Zero Shear Viscosity (ZSV) mixing and compaction temperatures were obtained by using a procedure developed during the NCHRP 9-10 project [4, 7]. The binders were tested at three temperatures: 165ºC, 135ºC and 105ºC. At each temperature, different shear rates were applied to the binder and the viscosity values registered. The shear rates ranged from 0.28 1/s to 93 1/s, covering all the range available in the testing machine. The lowest shear rate available by the instrument is not low enough to be representative of zero shear. To estimate the ZSV, the

recorded values at each temperature were fitted into a Cross Williamson (C-W) model with the help of a spreadsheet. The C-W model is presented in equation 1.1.

$$h = h_{\infty} + \frac{(h_0 - h_{\infty})}{1 + \left(k \frac{dg}{dt} \right)^n} \qquad \text{eq.1}$$

Where h is the viscosity, h_0 is the ZSV asymptote, $h_{¥}$ is the high shear viscosity asymptote dg/dt is the strain rate, k and n are model parameters. The ZSV were obtained by extrapolating to zero shear rates using the C-W model. An example of the fitted values for one of the samples (project# 1020-01-74, sample A) is shown in figure 1.1.

The mixing and compaction temperatures according to this procedure, are the ones that show a ZSV viscosity of 1.5 Pa·s and 3.0 Pa·s respectively. When the ZSV were obtained for each of the three temperatures (165ºC, 135ºC and 105ºC), interpolation was used to calculate the mixing and compaction temperatures. Two samples were tested for each binder to assure repeatability, which was chosen as ± 7ºC (approximate 5%). In case of discrepancy, a third sample was tested and the two closest values were reported.

The analysis of the data was found to be not an easy task. Using the described procedure and the available testing equipment (Brookfield Viscometer) a high degree of extrapolation is needed to find the ZSV. As mentioned before, the lowest shear rate available was 0.28 1/s. Shear rates that can realistically represent the ZSV are in the order of 0.001 1/s [7]. The amount of extrapolation required, in the opinion of the authors, makes the results questionable. This might be the reason why the ZSV mixing and compaction temperatures obtained for the binder 1170-13-70, PG64-34 were unreasonably high. Despite this fact, the results were reported and analyzed to verify the relationship between the laboratory data and the field data. Table 1.2

shows the ZSV mixing and compaction temperatures for each binder (average of the two tested samples).

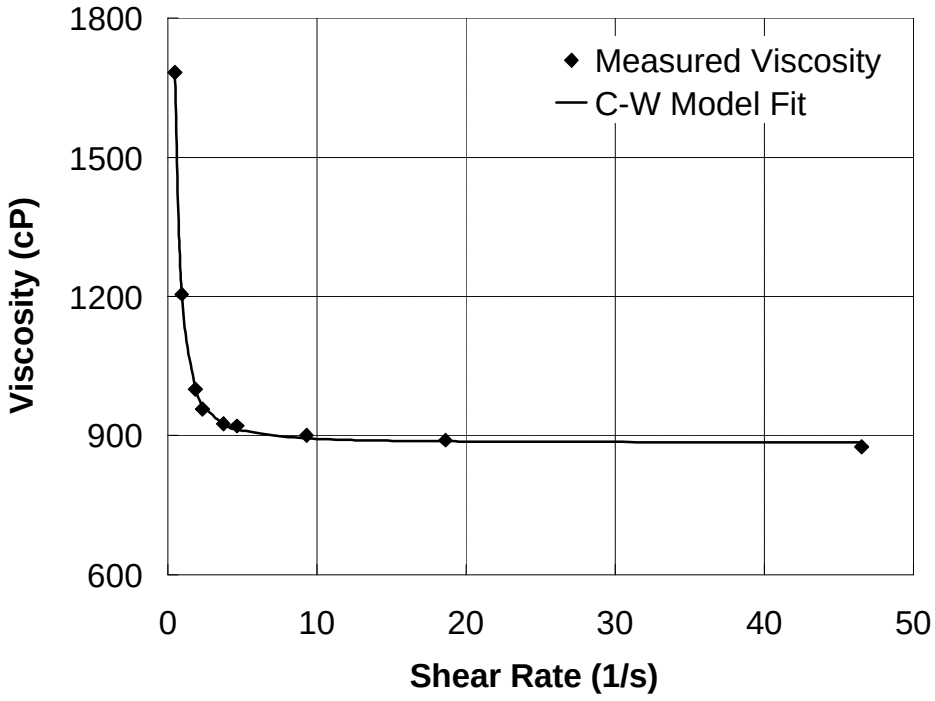

* 1000 cP = 1 Pa·s

FIGURE 1.1 Measured Viscosity Values and Fitted C-W Model for Sample A at 135ºC, Project #1020-01-74

The results of the binder testing show that in all cases (except in binder 1170-13-70, PG64-34) the temperatures obtained with the Superpave procedure are higher than the ZSV temperatures. This is observed in both, mixing and compaction temperatures. For five of the binders, the Superpave mixing temperatures were greater than 165ºC, which is excessively high and causes accelerated aging of the material [Sharp, 7]. These results have been reported before [7]. The ZSV mixing temperatures were all below 165ºC (except binder 1170-13-70, PG64-34). The mixing temperatures obtained by both methods were compared with the temperatures recommended by the providers of the HMA. Table 1.3 shows provider recommended mixing

temperatures, obtained from the mix design of each project and from direct communication with the mixing plants staff.

TABLE 1.3 HMA Provider Recommended Mixing Temperatures

DOT Project ID	Binder	Provider Recommended Mixing Temp.
9040-09-70	58 - 34	142 - 144
1020-01-74	70 - 28	N/A
7132-04-61	58 - 28	135 - 149
7132-04-61 (Inters.)	64 - 28	N/A
1170-13-70	64 - 34	135 - 149
7200-05-70	70 - 28	160*
20050412025 (contract #)	64 - 28	135 - 149
5300-04-74	64 - 28	157 - 163

* Temperature of the aggregates during mixing

By comparing tables 1.2 and 1.3, it can be observed that in general both methods predict temperatures higher than the recommended by the providers. However, the ZSV temperatures were closer to the provider temperatures in most cases. The only binder where both methods agreed with the provider recommended temperatures is the 7132-04-61 PG58-28. This result is expected, since the Superpave method was calibrated for non modified binders like this one.

For three of the projects (7200-05-70 PG70-28, 20050412025 PG64-28 and 5300-04-74 PG64-28) samples of mixture were prepared using the ZSV mixing temperatures. In all three cases, good coating of the aggregates was observed. These results confirm that the mixing temperatures recommended by Superpave are excessively high and not needed to achieve good mixing.

1.2 Field Compaction Data

1.2.1 Project Information and Compaction Data

Field compaction information was taken from four different HMA paving projects in Wisconsin. The sampling was done between Fall 2003 and Fall 2005. Mixture samples were taken directly in front of the paver. Binder samples were taken from the asphalt mixing plant. The information of the projects is given in table 1.4.

In the field, compaction data including temperature and density was taken during the paving process. Using an infrared gun, the surface temperature was measured and recorded after each roller pass. Density data was also taken after each roller using a nuclear gage. Only fifteen second reading was allowed for the nuclear gage reading, because of the short times between roller passes. For each project, the data was taken from two to four measuring points, depending on the feasibility. Tables 1.5 and 1.6 show the compaction data obtained for each project.

TABLE 1.4 Project and Sample Information

Project Name	DOT Project ID*	Layer	Binder	Polymer Modified	Mixture	Date Sampled
STH 17 Rhinelander Bypass	9040-09-70	Base	58 - 34	YES	E-3 19mm	Sep-03
I – 94 Baldwin	1020-01-74	Surface	70 - 28	YES	E-30 12.5mm	Oct-03
Hanley Rd. Intersection Hudson	7200-05-70	Surface	70 - 28	YES	E-10 19mm	Sep-05
Madison Beltline (Midvale-Gammon)	5300-04-74	Surface	64 - 28	YES	E-10 12.5mm	Oct-05

TABLE 1.5 Field Compaction Data for Projects 1020-01-74 and 9040-09-70

Project 1020-01-74, PG70-28, E-30 12.5mm, lift thickness = 2.5in										
Roller Type	Pass #	Location 1			Location 2 (Center)			Location 3		
		% Max. Density	Temp. ºC		% Max. Density	Temp. ºC		% Max. Density	Temp. ºC	
			Surf.	Ave.		Surf.	Average		Surf.	Average
Paver	1	70.3%	106	121	--	--	--	--	--	--
Pneumatic	1	77.0%	108	123	83.0%	106	121	78.0%	104	119
Breakdown	1	85.6%	99	113	87.9%	96	110	--	--	--
(Vibratory)	2	84.8%	96	110	87.1%	97	111	86.8%	95	110
Steel Roller	1	88.9%	66	78	90.2%	64	76	91.1%	65	77
(Vibratory)	2	88.4%	61	73	91.7%	55	66	90.4%	59	71
	3	89.7%	59	70	--	--	--	--	--	--
Cold	1	88.1%	52	63	92.9%	51	61	90.5%	52	63
(Vibratory)	2	90.1%	48	59	92.6%	48	58	91.3%	51	61
	3	87.5%	39	49	90.7%	43	53	90.8%	46	56
(Static) =>	4	--	--	--	90.8%	43	53	91.9%	42	52

Project 9040-09-70, PG58-34, E-3 19mm, lift thickness = 3 in													
Roller Type	Location 1				Location 2			Location 3			Location 4		
	Pass #	% Max. Density	Temp.ºC *		% Max. Density	Temp.ºC		% Max. Density	Temp.ºC		% Max. Density	Temp.ºC	
			Surf.	Ave.		Surf.	Ave.		Surf.	Ave.		Surf.	Ave.
Paver	1	73.7%	130	145	70.2%	128	143	74.0%	127	142	73.7%	127	142
Break	1	78.7%	104	116	--	--	--	--	--	--	--	--	--
Down	2	--	--	--	78.1%	103	115	--	--	--	--	--	--
(Vibratory)	3	85.8%	101	113	79.8%	78	89	--	--	--	--	--	--
	4	--	--	--	--	--	--	--	--	--	--	--	--
	5	87.9%	85	96	86.3%	77	87	86.5%	98	110	95.6%	85	96
	6	--	--	--	--	--	--	88.2%	82	93	92.1%	81	92
	7	--	--	--	--	--	--	89.6%	82	93	--	--	--
	8	--	--	--	--	--	--	90.0%	77	88	89.6%	77	88
	9	--	--	--	--	--	--	91.9%	72	82	92.5%	74	84
(Static)	10	--	--	--	--	--	--	--	--	--	92.0%	72	82

TABLE 1.6 Field Compaction Data for Projects 5300-04-74 and 7200-05-70

Project 5300-04-74, PG64-28, E-10 12.5mm, lift thickness = 1.75in							
Roller Type	Pass #	Location 1 (North)			Location 2 (South)		
		% Max. Density	Temperature ºC		% Max. Density	Temperature ºC	
			Surface	Average		Surface	Average
Paver	1	76.8%	129	144	78.7%	121	136
Breakdown	1	84.4%	110	124	87.6%	108.3	122
(Vibratory,	2	86.0%	102	115	--	--	--
Cold	1	86.3%	55	65	88.5%	56	66
	2	86.7%	54	64	87.8%	53	63
Project 7200-05-70 PG70-28, E-10 19mm, lift thickness = 3 in							
Roller Type	Pass #	Location 1 (North)			Location 2 (South)		
		% Max. Density	Temperature ºC		% Max. Density	Temperature ºC	
			Surface	Average		Surface	Average
Paver	1	70.7%	102	117	72.0%	111	126
Breakdown	1	81.7%	88	101	--	--	--
(Vibratory)	2	85.7%	82	95	85.0%	88	101
	3	87.2%	67	78	86.9%	88	101
	4	88.6%	82	95	87.1%	87	100
	5	88.8%	79	92	87.3%	79	92
	6	91.1%	81	94	89.5%	82	95
	7	88.7%	82	95	--	--	--
	8	91.5%	82	95	--	--	--
Pneumatic	1	91.9%	68	79	87.5%	73	85
(15 Ton)	2	88.8%	68	79	90.4%	72	84
	3	89.8%	67	78	91.0%	72	84
	4	90.8%	68	80	91.0%	72	84
	5	89.4%	69	81	88.4%	72	84
	6	94.6%	68	80	90.6%	72	84
	7	92.1%	68	80	89.4%	71	83
	8	89.9%	67	79	89.3%	71	83
	9	94.0%	65	76	89.5%	70	82
	10	93.3%	63	75	90.2%	69	80
	11	90.4%	62	73	90.4%	67	78
	12	94.0%	62	73	91.3%	67	78
	13	N/A	N/A	N/A	90.7%	68	79
Cold	1	92.4%	56	67	93.1%	56	66
(Vibratory)	2	93.5%	57	68	93.1%	56	66
	3	92.7%	52	62	92.5%	52	62
	4	--	--	--	92.4%	52	62
(Static) =>	5	--	--	--	92.6%	52	62

1.2.2 Field Compaction Temperatures

The temperatures shown in tables 1.5 and 1.6 correspond to mat surface temperatures and average mat temperature. The surface temperature was directly measured with an infrared device. However, the average temperature of the mat was not measured directly so it needed to be estimated. The average temperature of the asphalt lift is generally higher than the surface temperature and it depends on several factors like the air temperature, base temperature, mat thickness, wind and roller water. As an approximation, the average mat temperature after lay down can be estimated somewhere between 10ºC and 15ºC higher than the surface temperature (*11*, *12*). The initial temperature difference diminishes as the mat cools down (*13*). The lift thickness for the four projects varies between 1.75 in and 3 in, which are relative thick lifts. Considering the thickness, the average temperature was estimated as 15ºC higher than the surface temperature at the beginning of the compaction. Towards the end of the compaction, this difference was estimated to be 10ºC (*13*). Linear interpolation was used between these two numbers for intermediate temperatures. For all the analysis that follows, the average mat temperature was used.

It can be observed in tables 1.5 and 1.6 that the lay down temperature starts in the range 135ºC – 145ºC for projects 9040-09-070 and 5300-04-74, and in the range 115ºC – 125ºC for projects 7200-05-70 and 1020-01-74. It is interesting to notice that the two later projects have the stiffer asphalt binders (PG70-28) and have the lower lay down temperatures. The temperature for the first breakdown roller pass was between 115ºC and 125ºC for all projects except for project 7200-05-70, where it was close to 100ºC.

The compaction continued even for mat temperatures close to 60ºC. But the last roller passes are not for increasing the density, but for surface finishing with static rollers. Table 1.6 shows

that increases in density are observed in project 5300-04-74 with the vibratory breakdown roller, at mat temperatures between 115ºC – 125ºC. There was a big delay between the vibratory roller and the next roller that allowed the mat to cool down to the 60ºC – 70ºC range. It can be seen that this temperature was too low and no further increases in density were achieved. It should be noticed that the project was a warranty pavement, so no density requirements were specified by the DOT. Table 1.5 shows that for project 1020-01-74 increases in density are observed still with the second vibratory roller, at mat temperatures in the 70ºC to 80ºC range. However, when the last roller came, with mat temperatures in the 50ºC – 65ºC range, no further density increments were observed. For project 9040-09-70 the compaction was stopped around 80ºC, and it can be seen that increments in the density were observed until the last roller passes. Finally, for project 7200-05-70, increases in density are observed until temperatures in the 70ºC to 80ºC range, when the pneumatic roller is acting. For temperatures lower than this, no further densification was achieved.

In summary, densification was achieved in the projects until a limiting temperature was reached and or acceptable density was achieved. Below this critical temperature, more roller passes did not result in more density. The limiting temperature appears to be a number between 70ºC and 80ºC for the sampled projects. Figure 1.2 shows the densification data as a function of temperature for the four projects. For each project, the temperature and density displayed is the average of all the measuring locations at each roller pass. The figure could seem somewhat confusing since it shows increase in density with decreasing temperature. It should be realized, however, that the number of passes is increasing while temperature is decreasing and also air-void content is reducing significantly, resulting in more resistance to densification.

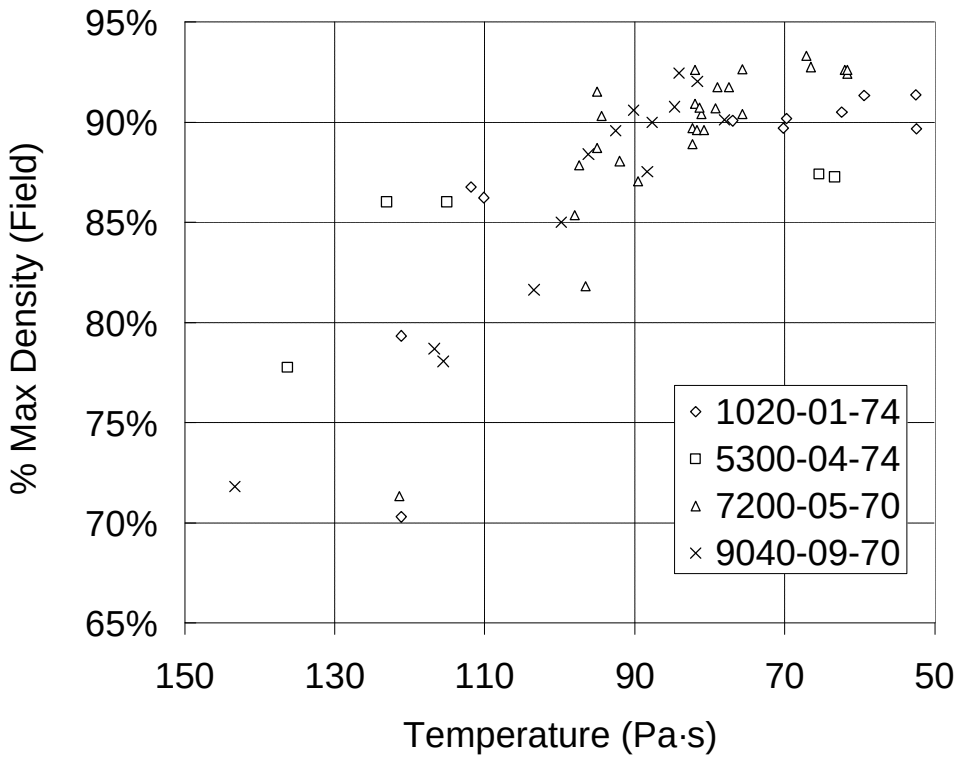

FIGURE 1.2 Field Density v/s Temperature, All Projects

1.2.3 Rollers Contact Pressure

The contact pressure of the rollers is not a constant value, and it varies during the compaction process. For steel rollers, the factors that affect the contact pressure are the roller weight, the drum diameter, the vibration and the penetration of the drum into the HMA mat (*1*). For the pneumatic rollers, the contact pressure is given by the tire pressure, which is typically in the range of 550 to 600 kPa (*1*). Figure 1.3 shows the schematics of the mat compaction that allow to calculate the contact pressure for a steel roller.

The vertical force is equal to the roller weight. The contact area is calculated from the drum geometry and penetration in the mat. The contact area A is given by equation 1.2.

$$A = a \cdot r \cdot L = \text{acos}\left(\frac{r + h_2 - h_1}{r}\right) \cdot L \qquad \text{eq.1.2}$$

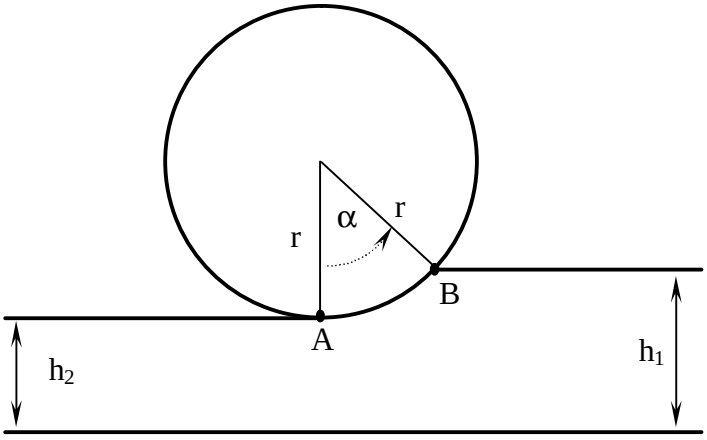

h_1 = mat height before roller pass

h_2 = mat height after roller pass

r = radius of steel drum

α = angle between contact points A and B in (rad)

FIGURE 1.3 Schematics of the Mat Compaction

Where L is the drum width, while α, r, h_1 and h_2 are defined in figure 1.3. The contact pressure is calculated by dividing the roller weight by the contact area A. Using this procedure, the contact pressures were estimated for the compaction processes of the four projects included in the study.

The first step corresponds to the estimation of the drum penetration in the mat ($h_1 - h_2$). This value can be calculated using the lift thickness and the difference in density before and after each roller pass. The penetration is approximated by equation 1.3.

$$h_1 - h_2 = (D_2 - D_1) \cdot t \qquad \text{eq.1.3}$$

where: $h_1 - h_2$ = drum penetration in the mat

D_1 = %max density before the roller pass

D_2 = % max density after the roller pass

t = lift thickness

To calculate the vertical loads, standard rollers used in the current practice were used. The breakdown and vibratory rollers were assumed to be 15 tons with a drum diameter of 60 inches. The cold roller was assumed to be 10 tons with a drum diameter of 60 inches. Using this information, together with equations 1.2 and 1.3 and the data from tables 1.5 and 1.6, the penetrations were calculated for the rollers during the compaction process of each project. The contact pressures can then be obtained from the penetration values obtained and the roller types selected. Table 1.7 shows the contact pressure for project 1020-01-74 (negative values are not included).

TABLE 1.7 Contact Pressure for Project 1020-01-74 (PG70-28, E-30 12.5mm, lift thickness = 2.5in)

Roller Type	Pass #	Average Temp. ºC	Density Increase %	Penetration (in)	Contact Pressure (kPa)
Paver	1	117	--	--	--
Neumatic	1	117	9.0%	0.23	600
Breakdown	1	109	7.4%	0.19	385
(Vibratory)	2	107	-0.5%	-0.01	--
Steel Roller	1	76	3.8%	0.10	625
(Vibratory)	2	70	0.1%	0.00	690
	3	70	-0.5%	-0.01	--
Cold	1	63	0.8%	0.02	650
(Vibratory)	2	60	0.8%	0.02	650
	3	53	-1.7%	-0.04	--
(Static) =>	4	54	1.7%	0.04	650

Based on analyzing the data for all the projects, it is observed that the estimated contact pressure for the breakdown roller started at approximately 300 kPa – 400 kPa and reached the range of 600 kPa – 700 kPa, after two or three passes. This is expected because the densification is higher at the beginning of the compaction, so the penetration and the contact area are bigger. The intermediate and cold rollers showed contact pressures in the range of 600 kPa – 700 kPa. This is also expected because they do not add density to the mat at very high rates, so the penetrations and contact areas are smaller. It is interesting to notice that the original intention of the Superpave Gyratory Compactor (SGC) pressure was to simulate the tire pressure of the trucks during the service life of the pavement (*13*). The field data presented indicates that the 600 kPa also agrees well with the contact pressure the rollers give to the asphalt mat during most of the compaction process.

1.3 Binder Testing

1.3.1 Zero Shear Viscosity and Superpave Compaction Temperatures

In order to compare the field compaction data with some of the current specifications and recommendations for compaction, the compaction characteristics of the mixtures were studied at the Zero Shear Viscosity temperatures and the Superpave requirement temperatures. To determine the compaction temperatures, the binders were tested using a Brookfield viscometer model DV-II. The Superpave compaction temperature is the one at which a viscosity of 0.28 Pa·s (±003) is reached. Two samples were tested for each binder to assure repeatability. Table 1.8 shows the estimated Superpave compaction temperatures for the four projects.

The Zero Shear Viscosity (ZSV) mixing and compaction temperatures were obtained by using a procedure developed during the NCHRP 9-10 project (*4, 7*). The binders were tested at three temperatures: 165ºC, 135ºC and 105ºC. At each temperature, different shear rates were applied to the binder and the viscosity values registered. The shear rates ranged from 0.28 1/s to 93 1/s, covering all the range allowable by the testing device. The lowest shear rate allowable by the instrument is not low enough to be representative of zero shear. Extrapolation using a Cross Williamson (C-W) model was used, as suggested in NCHRP 459 report (*7*). The compaction temperature according to this procedure, is the one at which a ZSV of 3.0 Pa·s is achieved. Table 1.8 shows the ZSV compaction temperatures for each binder.

TABLE 1.8 Superpave and ZSV Compaction Temperatures

Project ID	Binder	ZSV Compaction Temperatures* ºC			Superpave Compaction Temperatures* ºC		
		Sample A	Sample B	Average	Sample A	Sample B	Average
9040-09-70	58 - 34	137.4	138.4	138	144.3	144.4	144
1020-01-74	70 - 28	151.1	148.4	150	162.8	162.3	163
7200-05-70	70 - 28	149.1	151.8	150	169.8	169.9	170
5300-04-74	64 - 28	137.7	137.6	138	154.6	154.2	154

* Average value. The temperature range is about ±10% off this value.

The compaction temperatures obtained using the ZSV or Superpave methods were higher than 135ºC for all projects. These values are not realistic compared to the field data. The compaction process in the field happened between 125ºC and 60ºC for the four selected projects. It was therefore decided that a new set of viscosity measurements be conducted to evaluate viscosities at actual field conditions.

1.3.2 Binders' Viscosities as a Function of Temperature

In order to study the influence of the binder viscosity in the compaction process, asphalt samples were tested at temperatures within the compaction range. Six different temperatures were chosen, with 15ºC spread: 135ºC, 120ºC, 105ºC, 90ºC, 75ºC and 60ºC. Shear creep test in the Dynamic Shear Rheometer (TA Instrument AR2000) was used to determine the steady state viscosity of the binders. Two different geometries were used for the test: parallel plate and cone and plate. Parallel plate was chosen because it is the most used geometry in asphalt rheology. Two different plate sizes were used: 25 mm (for 60ºC and 75ºC) and 40 mm (for the rest of the temperatures). Cone and plate geometry was used to verify the results. Modified binders are highly stress sensitive, and parallel plate geometry does not provide a constant strain rate through the sample. Cone and plate testing applies a constant strain rate in the sample. The cone used was

40 mm in diameter with 2º angle. For all creep tests, a low stress level was used, between 0.1 and 5 Pa, to ensure linearity and to achieve the low shear viscosity asymptote.

The results of both geometries showed good agreement. The results were also compared with the viscosities obtained at low shear rates using the Brookfield Viscometer and good agreement was also found. Figures 1.4 shows the viscosities from the three test methods for binder 7200-05-70 (PG70-28). For the four binders, power law correlations were fitted to the testing results, determining the temperature – viscosity relationship for the range of interest. Table 1.9 shows the fitted data for all binders.

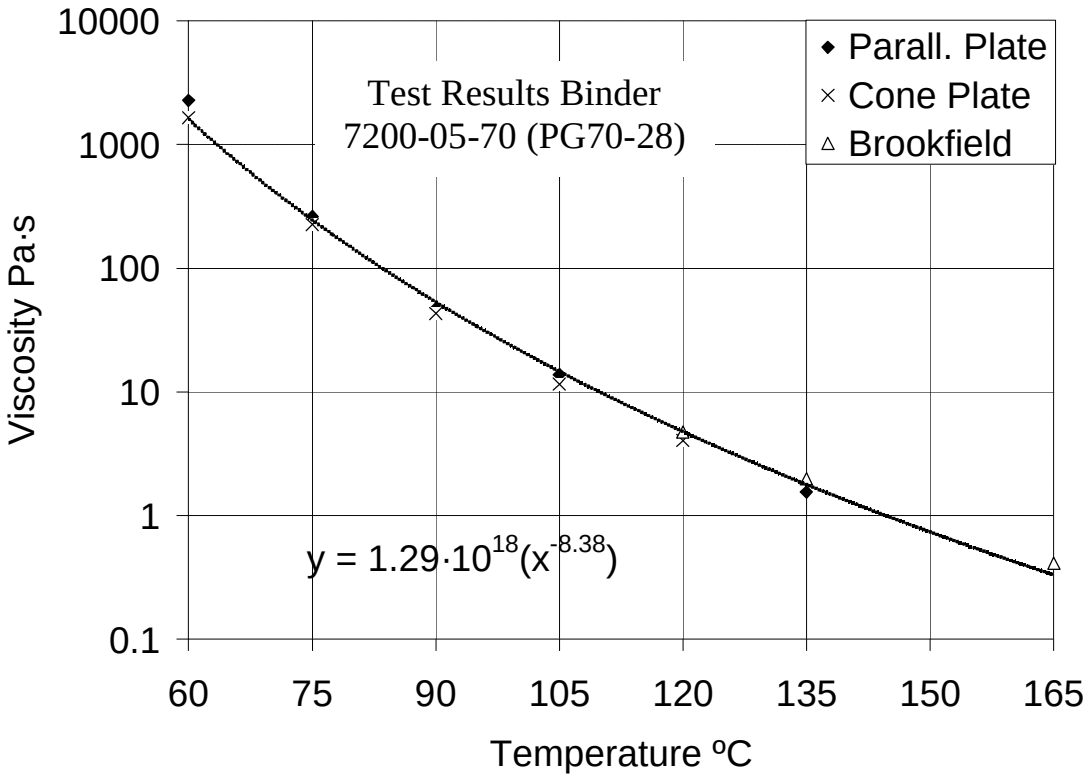

FIGURE 1.4 Viscosity Versus Temperature for binder 7200-05-70 (PG70-28)

TABLE 1.9 Fitted Viscosities for All Binders

Temperature (T) ºC	Fitted Viscosities (η) Pa·s			
	9040-09-70 (PG58-34) $\eta = 1.43 \cdot 10^{15} \cdot T^{-7.31}$	5300-04-74 (PG64-28) $\eta = 1.09 \cdot 10^{17} \cdot T^{-8.08}$	1020-0174 (PG70-28) $\eta = 2.12 \cdot 10^{18} \cdot T^{-8.55}$	7200-05-70 (PG70-28) $\eta = 1.29 \cdot 10^{18} \cdot T^{-8.38}$
60	144	468	1328	1621
75	28	77	197	250
90	7.4	18	41	54
105	2.4	5.1	11	15
120	0.90	1.7	3.5	4.9
135	0.38	0.67	1.3	1.8
150	0.18	0.28	0.53	0.75
165	0.09	0.13	0.23	0.34

1.4 Mixture Testing

The Superpave Gyratory Compactor (Pine Instrument, AFGC125X) was used to compare the densification properties of the mixes at conditions similar to the field conditions in terms of temperature and pressure. The compaction temperatures estimated according to the Superpave and ZSV criteria were also included in the testing plan. As discussed before, during initial breakdown, the contact area is bigger and so the contact pressure is smaller. For this reason, a lower compaction pressure of 300 kPa was considered for the temperature range where breakdown was observed in the field (120ºC and 105ºC). The rest for the compaction process happens at higher compaction pressures because of the lower contact areas. So for the lower temperatures only the standard 600 kPa was used, which is a good representation of the compaction pressures in the field as discussed earlier in this paper. The detail of the testing conditions considered is:

- 300 kPa of pressure at 120ºC and 105ºC

- 600 kPa of pressure at Superpave Temperature, ZSV Temperature, 120ºC, 105ºC, 90ºC, 75ºC and 60ºC

The results of the laboratory compaction were analyzed in terms of the %Gmm (percentage of maximum specific gravity) achieved at different levels of gyrations: %Gmm at N_{ini} (initial number of gyrations), N_{des} (design number of gyrations) and N_{max} (maximum number of gyrations). Projects 5300-04-74, 1020-01-74 and 7200-05-70 have the same Nini (8), Ndes (100) and Nmax (160), according to the Wisconsin DOT Standards (*15*). Project 9040-09-70 (E-3 mixture) corresponding compaction gyrations are 7 (Nini), 75 (Ndes) and 115 (Nmax), according to the WisDOT standards (*15*). Tables 1.10 includes the laboratory compaction results for project 1020-01-74 at different temperature and pressure combinations.

TABLE 1.10 Compaction Parameters for Project 1020-01-74 74 (PG70-28, E-30 12.5mm)

Sample ID	%Gmm N_{ini}	%G_{mm} N_{des}	%G_{mm} N_{max}
120ºC, 300 kPa – A	80.0%	89.4%	91.0%
120ºC, 300 kPa – B	80.1%	89.7%	91.3%
105ºC, 300 kPa – A	78.7%	87.9%	89.4%
105ºC, 300 kPa – B	81.1%	90.5%	92.0%
163ºC, 600 kPa – A	84.1%	94.2%	95.6%
163ºC, 600 kPa – B	83.5%	93.9%	95.4%
150ºC, 600 kPa – A	84.0%	94.4%	96.0%
150ºC, 600 kPa – B	83.6%	94.1%	95.7%
120ºC, 600 kPa – A	83.8%	94.3%	95.7%
120ºC, 600 kPa – B	83.7%	94.2%	95.7%
105ºC, 600 kPa – A	83.3%	93.6%	95.0%
105ºC, 600 kPa – B	83.7%	93.9%	95.4%
90ºC, 600 kPa – A	81.2%	91.5%	93.0%
90ºC, 600 kPa – B	82.8%	93.2%	94.7%
75ºC, 600 kPa – A	81.9%	92.4%	94.0%
75ºC, 600 kPa – B	82.2%	92.5%	94.0%
60ºC, 600 kPa – A	79.9%	90.5%	92.1%
60ºC, 600 kPa – B	79.4%	90.1%	91.7%

The influence of the compaction stress was analyzed by comparing the difference in the %Gmm between samples compacted at the same temperature. The data from table 1.10 shows

that the differences in %Gmm between samples compacted at the same temperature but different stress is about 4%. Figure 1.5 shows the compaction curves at 120ºC for project 7200-05-70. It can be observed that at the end of the compaction, the difference in %Gmm is also about 4%. To further evaluate the influence of stress, statistical analysis of variation with 95% confidence was used. For all project and for both temperatures considered, it is found that in all cases changing the stress level from 600 kPa to 300 kPa has a significant effect on the densification of samples. The comparison between the effects of stress level and temperature is presented in Figure 1.5 for project 7200-05-70. As shown, decreasing the stress from 600 kPa to 300 kPa has a much bigger effect in the densification than changing the temperature from 120ºC to 90ºC.

The data from table 1.10 shows that when the temperature is decreased from 163ºC to 75ºC, the %Gmm gradually decreases. However, when the temperature reaches 60ºC, the %Gmm reduces dramatically. The %Gmm at Nmax varies between 95.5% and 94% in the temperature range between 163ºC and 75ºC (600 kPa). But the %Gmm at Nmax for 60ºC is about 92%.

Figure 1.6 depicts this trend in a more clear way. It shows the %Gmm at Nini in all the temperature range for projects 9040-09-70 and 5300-04-74 (average of the two tested samples for each condition). It can be observed that for project 9040-09-70 there is a significant drop in the %Gmm for the 60ºC samples. For project 5300-04-74 , however, this drop in %Gmm appears to happen for the samples compacted at 75ºC. This result is expected, since the binder of project 5300-04-74 (PG64-28) is stiffer than the binder of project 9040-09-70 (PG58-34), so the former has a higher viscosity than the latter at 75ºC. This observation suggests that there is a limiting viscosity for the densification, above which the densification process is significantly affected.

The results from the laboratory compaction agree with what was observed in the field. As shown in figure 1.2, the field densification by rolling was achieved until temperatures in the 70ºC

– 80ºC range. No further densification was achieved for temperatures below this range. The lab densification showed a significant drop when samples were compacted at 75ºC or 60ºC. The exact limit of temperature for achieving compaction logically depends on the binder viscosity. Since temperature is not a material property, viscosity limits (as material properties) should be established as will be discussed next.

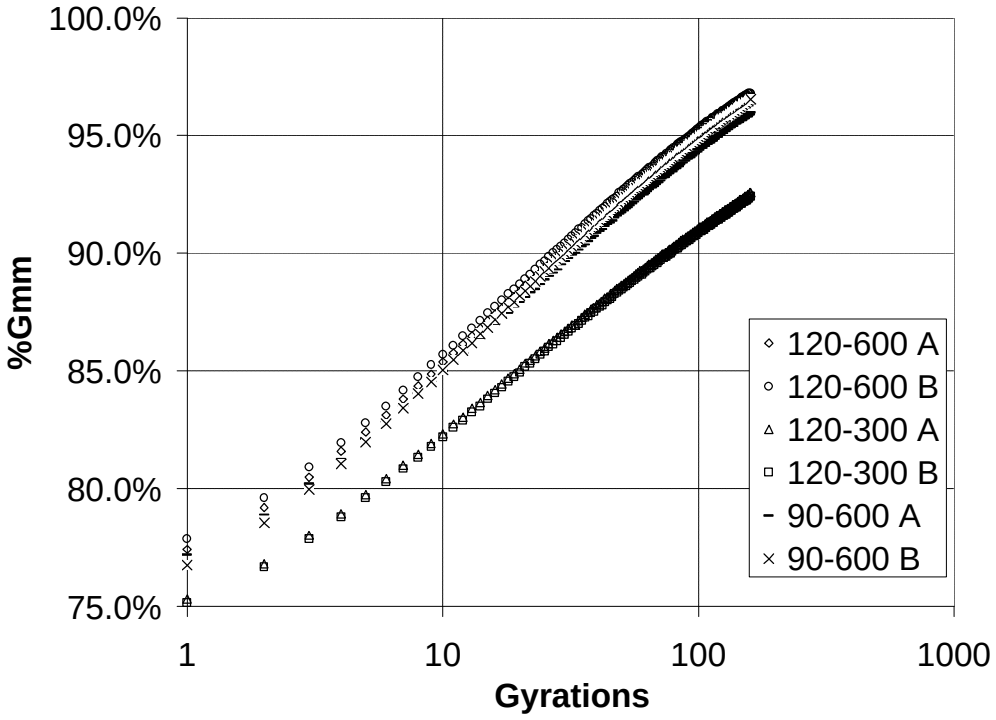

FIGURE 1.5 Compaction Curves Project 7200-05-70, 120ºC and 90ºC

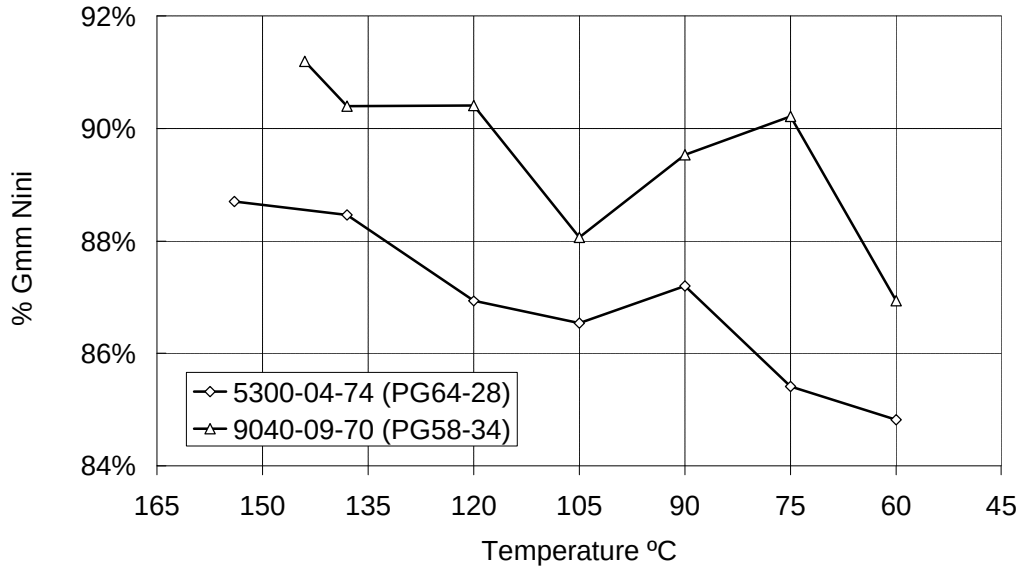

FIGURE 1.6 %Gmm at Nini versus Temperature Mixtures for Projects 5300-04-74 and 9040-09-70 (600 kPa)

1.5 Analysis of Field and Lab Compaction

Analyzing the influence of the binder viscosity in the field compaction is one of the main interests of this study. For this purpose, the viscosities of binders at the field mat temperatures (from Tables 1.5 and 1.6) were determined using the fitting functions from table 1.9, for each one of the projects, and a relationship between the field density and the binder viscosity was obtained. But more relevant than the density at each viscosity level, is the increase in density per roller pass at each viscosity level. The density increase can be calculated by subtracting the density before each roller pass from the density after the roller has gone over the mat, as shown in table 1.7. In other words, if the density after the second roller pass were (for example) 75% of the maximum density, and the density after the third roller pass were 80% of the maximum

density, then the increase in density with the third roller pass will be 5%. This increase in density was calculated for different viscosity ranges.

The binder viscosity in the field compaction temperature range was divided into different intervals, and the average increase in density per roller pass was calculated for each viscosity interval. Figure 1.7 shows the viscosity ranges and the average increase in field density for each interval. By looking at the chart, it can be seen how for viscosities higher than 100 Pa·s, very low compaction was achieved per each roller pass, compared with the densification achieved for viscosities lower than 100 Pa·s. From the field data, the limit seem to be a viscosity close to 100 Pa·s. Further analysis was carried out by fitting an exponential curve to the data of figure 6. The exponential fit is shown in the plot and it suggests the same lower viscosity limit of 100 Pa·s for compaction.

The observations from the above analysis of field data were contrasted with the lab compaction data. The viscosity temperature functions from table 1.9 were used to correlate the %Gmm at different gyration numbers in the SGC with the binder viscosity. Figure 1.8 shows the % Gmm at Ndes for the four projects versus the binder viscosity. It can be observed that the viscosity limit of 100 Pa·s seem to be working well only for mixtures of project 7200-05-70 (PG70-28). For the rest of the projects, this limit seems to be too high, since decreases in density are shown at lower viscosities. Mixtures from Projects 9040-09-70 (PG58-34) and 5300-05-070 (PG64-28) show a decrease in the %Gmm at Ndes for viscosities higher than 30 Pa·s. Mixture from Project 1020-01-74 (PG70-28) shows an initial decrease in densification for viscosities higher than 10 Pa·s, but the final sharp decrease happens for viscosities higher than 100 Pa·s. The same behavior was observed when the %Gmm at Nini and Nmax trends were analyzed.

Based on the density trends observed in figure 1.8, it appears that a viscosity limit should be a number in the range of 10 Pa·s to 100 Pa·s. The importance of the viscosity limit is that it could be translated into a temperature limit, which can be monitored easily in the field, and under which no more densification can be achieved in the field. The lower the viscosity limit, the higher the compaction temperature limit, so the more conservative the approach. Table 1.11 shows the limiting temperatures for the four projects considered in this study, using three different values of viscosity limit: 10 Pa·s, 50 Pa·s and 100 Pa·s.

Field Viscosity Intervals and Average Increase in field Density (All Projects)

Interval	Viscosity Range Pa·s	Average Increase in Field Density
1	1 – 3	3.6
2	3 – 9	3.3
3	9 – 27	1.6
4	27 – 81	2.4
6	81 – 243	0.6
7	243 – 729	0.4
8	729 – 2187	0.2
9	2187 – 6561	0.01

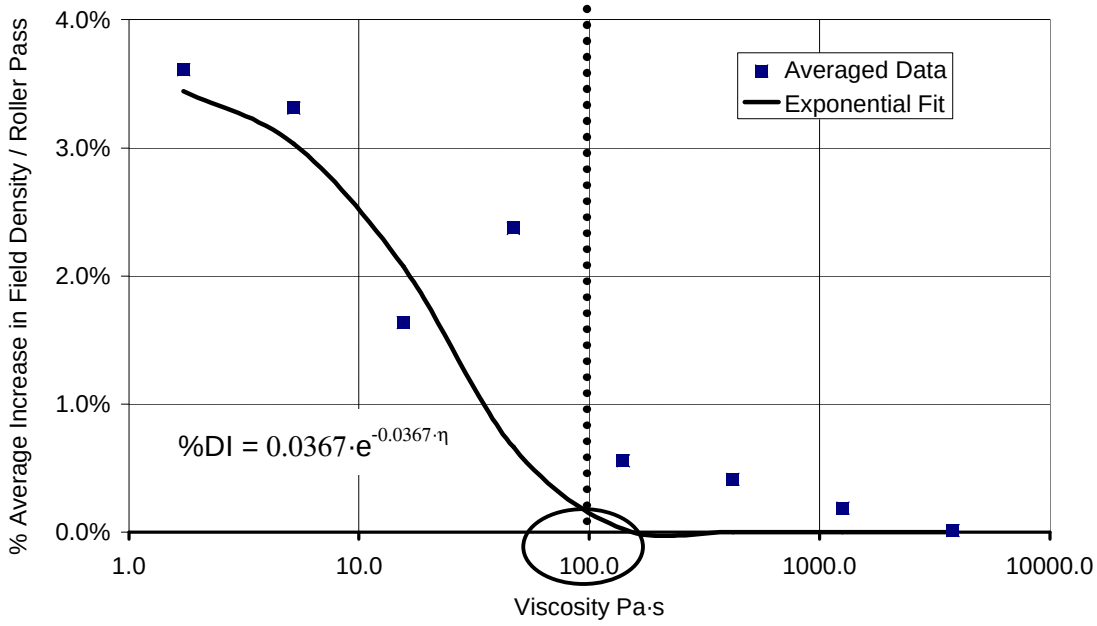

FIGURE 1.7 % Density Increase (%DI) versus Binder Viscosity (Field Data)

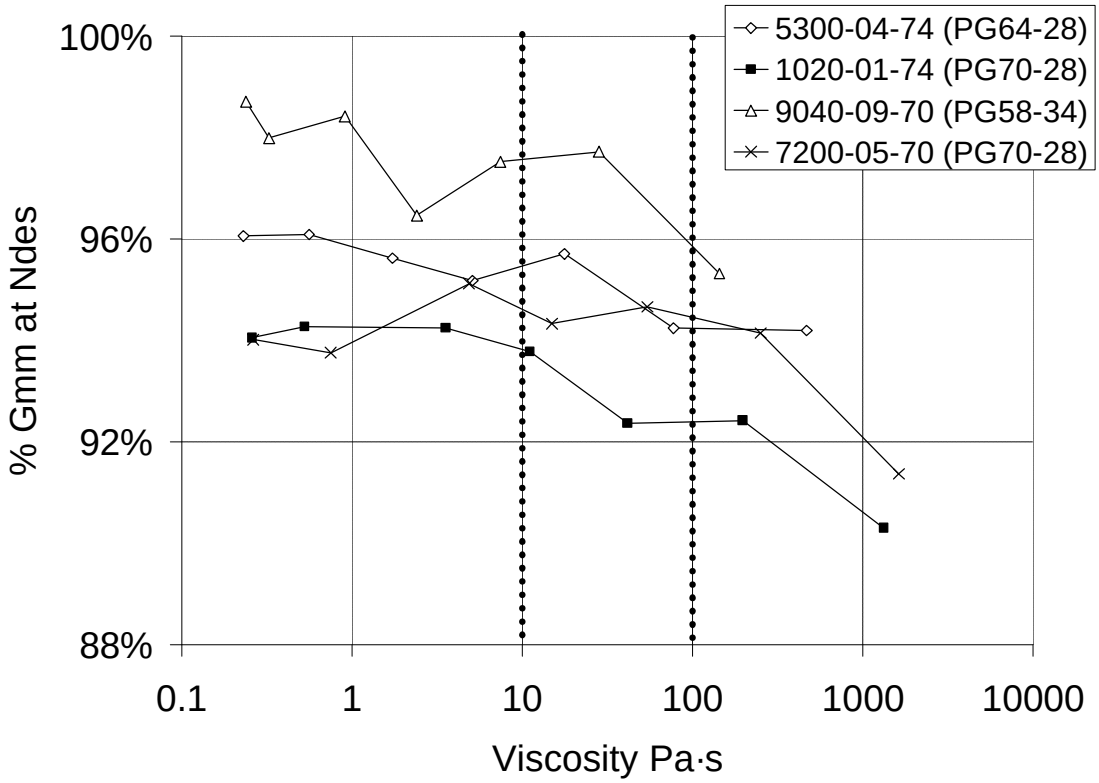

b)

FIGURE 1.8 %Gmm at Ndes versus Binder Viscosity (Lab Data)

TABLE 1.11 Temperature Limits for Compaction based on different Low Shear Viscosity Limits

Project	Temperature Limit for Compaction		
	Visc. Limit = 100 Pa·s	Visc. Limit = 50 Pa·s	Visc. Limit = 10 Pa·s
9040-09-70 (PG58-34)	63 ºC	69 ºC	86 ºC
5300-04-74 (PG64-28)	73 ºC	79 ºC	97 ºC
1020-01-74 (PG70-28)	81 ºC	88 ºC	106 ºC
7200-05-70 (PG70-28)	84 ºC	91 ºC	110 ºC

By comparing the different temperature limits from table 1.11 with the field compaction data from tables 1.5 and 1.6, some conclusions can be obtained.

- The viscosity limit of 10 Pa·s seem to be unreasonably conservative, since it specifies a temperature lower limit for compaction equal to 110 ºC for project 7200-05-70 (PG70-28). The field data from table 2 indicates that the breakdown compaction for project 7200-05-70 started around 100ºC and adequate compaction was achieved at this range.
- The viscosity limit of 100 Pa·s gives reasonable temperatures for three of the projects, but would result in a temperature limit of 63ºC for project 9040-09-70 (PG58-34) which seem too low and unreasonable.
- An intermediate value of 50 Pa·s seem to be a reasonable choice. The temperature limits for the four projects obtained based on 50 Pa·s are still high compared with the field data, which makes this number a conservative choice.

1.6 Suggested Procedure For Determining Compaction Temperatures

Compaction in the field happens at much lower temperatures than the ones predicted with the current methods, which makes the estimation of temperatures based on current criteria meaningless. Since the binder and aggregates still need to be heated in order to be mixed, the high initial temperature of the compaction is already guaranteed. But the missing item in the current specifications is the determination of the lower temperature limit where densification can be achieved. According to the present study, it appears that the temperature at which the binder viscosity is equal to 50 Pa·s is a reasonable limit above which significant reduction in densification rate is observed. The limit presented here is based on low shear rates viscosity. For the binders tested in the present study, it was observed that the plateau for the low shear rate

asymptote was reached for shear rates below 0.5 1/s. For the temperature range below 90ºC, this shear rate could be achieved with stresses below 5 Pa for the creep test. A tentative procedure is suggested below to determine the viscosity limit.

- Perform a Creep test at with the DSR using parallel plate geometry
- Use three different temperatures: 60ºC, 75ºC and 90ºC
- Use a shear rate below 0.5 1/s, which can be normally achieved with a creep stress below 5 Pa.
- Each creep test should last at least 45 minutes to reach equilibrium. The average viscosity of the last five minutes of reading is recorded as the steady state viscosity.
- Use at least 15 minutes of sample temperature equilibrium between creep tests
- After the viscosities are calculated for the three temperatures, obtain a power curve fitting for the viscosities using a spreadsheet.
- Using the fitting equation, calculate the temperature at which the viscosity is equal to 50 Pa·s, which will be equal to the minimum temperature limit for compaction.

1.7 Summary of Findings Mixing and Compaction Study

Based on the data collected and analysis of the results the following summary of findings could be stated:

- The compaction process in the field projects of this study happened at temperatures between 125ºC and 60ºC. The majority of densification is achieved, however, at temperatures above the 80ºC range. The last roller passes, which are done at lower temperatures, are generally for surface finishing only. It is recognized that there are 3

temperature zones during compaction: temperatures that are too high resulting in spider cracking of the HMA mat, optimum temperature for compaction, and transition or tender temperature zone. In this project the focus was only on optimum temperatures and cooling to the end of finishing. In the laboratory, using the SGC, the tender zone effect could not be observed possibly due to the high confinement of the gyratory compactor.

- There appears to be no good relationship between the compaction temperatures recommended by the current specification methods (using 0.28 Pa-s viscosity) and the effectiveness of the compaction in the field. It seems that a new higher level of viscosity and a lower limit for the compaction temperature can be established to allow a wider compaction window of time and lower need for heating.
- A similar conclusion can be obtained from the lab compaction data. The %Gmm curves did not reduce dramatically when the temperature was reduced to approximately 75ºC, for the mixes of this study. When the temperature was decreased below this limit, however, significant decreases in the %Gmm curves were observed. The specific temperature lower limit depended on the binder viscosity.
- The rollers contact pressures seem to vary between 300 kPa and 700 kPa during the compaction process. The breakdown rolling occurs at contact pressures between 300 kPa and 400 kPa. After a few rolling passes, the contact area decreases increasing the contact pressure to values between 600 kPa and 700 kPa. This shows that the current standard pressure of the SGC is a good estimate of the contact pressures at which the most of the compaction happens in the field.
- The compaction pressure has a significant effect on the densification of the samples tested in the lab. Since the breakdown rolling happens at lower contact pressures, it is important

that the breakdown rolling happens at high asphalt mat temperatures, not too long after the paver.

- The field and lab data for the four projects analyzed, indicated that the low temperature limit for compaction can be estimated using a low shear viscosity limit of 50 Pa·s at 0.5 (1/s). The DSR with parallel plate geometry can be used to measure this temperature.
- The fact that densification happens successfully at such low temperature ranges indicates that there is probably a big influence of the stress sensitivity of the binders on the compaction process. When the temperature is dropped from 135ºC to 90ºC the viscosity of the binder can increase between 20 and 30 times. The fact that this does not have a very big effect in the densification suggests that the roller pressures, and SGC stresses, are high enough to cause shear thinning in the binders and generate densification nonetheless. This effect needs further research.
- One of the limitations of the work presented here is that it considers only the binder viscosity and neglects the effect of the aggregate interlock in the compaction process in order to simplify the analysis and to estimate the lower temperature limit for compaction. The other limitations are the small size of the projects visited and the relatively narrow range of temperatures covered in these projects.
- The study shows that compaction in the field is done at temperatures much lower than what has been commonly used in the laboratory. It also shows that the Gyratory compactor can be used at much lower temperatures than commonly used and that density can still be achieved at relatively high viscosities. The results confirm the concerns expressed by some practitioners that mixtures are being overheated and that the need for low viscosities is possibly over emphasized. The results cover a relatively small set of

field projects and the recommended procedure is proposed as a starting point to change thinking about compaction temperatures. There is no doubt that energy and pollutants could be reduced when lower compaction temperatures are used. It is however also true that if temperatures are too low, density might not be achieved. Defining the optimum temperature range to reduce heat energy consumption and achieve density is a difficult but achievable task. Developing reliable laboratory methods to have accurate estimates of the optimum temperature zone is needed.

- The mixing temperatures using the ZSV protocol seem to be adequate for the HMA mixing. The current tools to estimate ZSV from the Brookfield viscometer data, however, did not seem totally reliable. The extrapolation required from the shear rates available from the viscometer can add significant error in the estimations.

CHAPTER TWO: FATIGUE

2.1 Background

This section of the report deals with the field validation of the fatigue specifications for modified binders proposed in the report 0092-01-01 Development of Guidelines for PG Binder Selection in Wisconsin [16]. The new parameter for evaluating the fatigue life is called N_{P20}, and it is obtained by time sweep testing at the average pavement temperatures expected on the site. The details of the testing procedure are described in detail on the literature [7, 16]. The summary of the binder specifications for fatigue developed previously [16, 17] are described in the present section.

For a specific binder and temperature, N_{P20} is a function of the input energy used in the testing, known as "Wi". The required input energy was previously defined for the yearly average pavement temperature in Wisconsin. Table 2.1 shows the input energy values recommended for different pavement structures [16] and two different temperatures.

TABLE 2.1 Input Energy Wi in Pa (8ºC and 13ºC)

Temp. ºC	Major Highway	Médium Highway	Minor Road	Major Urban	Medium Urban	Minor Urban
8	800	4000	13000	800	3000	10000
13	500	2500	6500	500	2000	5000

In order to determine which Wi should be used to calculate N_{P20}, the pavement needs to be categorized into one of the six categories shown in table 2.1. Once the input energy is determined, the N_{P20} value can be determined for the binder and compared with the specified minimum N_{P20}. The suggested limits for the fatigue parameter N_{P20} are a function of the traffic volume only and are presented on table 2.2. The concept represented by the N_{P20} parameter

implies that the testing conditions represented by Wi and temperature vary for each binder depending on the pavement and weather conditions. But the N_{P20} limits required are function of the traffic volume only.

TABLE 2.2 Recommended Np20 Limits

Traffic Volume (million ESAL)	Minimum N_{p20}
0 - 0.3	1500000
0.3 - 1.0	5000000
1.0 - 3.0	15000000
3.0 - 10	50000000
10.0 - 30.0	150000000
> 30.0	500000000

2.2 Selected Projects

Eight different projects were selected for the validation of the fatigue parameter N_{P20}. The description of the projects is presented in table 2.3. Seven of the projects used PMA binders, with three different PG grades (PG58-34, PG64-28 and PG70-28). One project that used a neat binder (PG64-22) was selected for comparison. The project traffic data and design life is presented in table 2.4. By looking at the project design ESALs and the design speed, the pavements were divided into the categories specified in table 2.1. Projects with design ESALs lower than 1 million were assumed to be minor roads (or urban). Projects with design ESALs between 1 million and 10 millions were considered medium highway (or urban). When the design ESALs was higher than 10 million, the project was characterized as a major highway (or urban). The project plan was not available in the WisDOT database for project 3120-06-70, so no traffic data could be gathered. Since the material information for the project indicated that an E-1 mixture was used for the surface layer, it was categorized as a minor road.

TABLE 2.3 Project and Sample Information

Project Name	DOT Project ID*	Binder	Polymer Modified	Construction Year
STH 17 Rhinelander Bypass	9040-09-70	58 - 34	YES	2003
Charlotte Court - Clover Road (STH 64)	9140-07-70	58 - 34	YES	2003
South County Line - CTH M (USH 51)	1177-10-70	58 - 34	YES	2003
Pine, Main & Mill Streets City of Weyauwega (STH 110)	6590-00-70	64 - 28	YES	2003
De Pere-Green Bay-Lombardi Ave - IH 43 (USH 41)	1130-12-71	64 - 28	YES	2003
STH67 – Walworth County	3120-06-70	64 - 28	YES	2003
Calumet Ave., City of Manitowoc (USH 151)	4100-10-71	64 – 22	NO	2003
Airport Freeway (IH 894)	1090-14-70	70 – 28	YES	2003

* Refers to the project # assigned by the Wisconsin DOT

TABLE 2.4 Traffic Data and Design Life

Project ID	Design ESALs	Growing Rate (Linear)	Design Life (years)	Design Speed (mph)	Category
9040-09-70	2029400	2.4%	20	60	Medium Highway
9140-07-70	1511101	1.5%	20	55	Medium Highway
1177-10-70	1898000 (1423500)	1.5%	20	55 (30-45)	Medium Highway (Medium Urban)
6590-00-70	861000	2.0%	20	30 - 40	Minor Urban
1130-12-71	19388800	2.1%	20	70	Major Highway
3120-06-70	> 1000000	1.7%	N/A	(rural)	Minor Highway
4100-10-71	4600000	1.5%	20	35	Medium Urban
1090-14-70	15972400	1.6%	20	60	Major Highway

2.3 Binder Testing

2.3.1 Time Sweep and N_{P20}

The binders were aging using the RTFO before testing. The temperature for testing was selected as 15ºC for all binders, which is the yearly average pavement temperature in Wisconsin. Two levels of input energy were chosen for the testing. One level slightly above the linear range of the binder, and one level approximately 75% of that value. The results for the binder testing are presented in table 2.5. After the values of N_{P20} are determined for the two selected stress levels, the parameters of the relationship between N_{P20} and Wi (K1 and K2) can be calculated, as shown in equation 2.1. The values obtained for K1 and K2 are shown in the last columns of table 2.5.

$$N_{p20} = K1 \cdot Wi^{-K2} \qquad \text{eq. 2.1}$$

Using the pavement structure categories defined on table 2.7 for each project, the input energy required can be selected from table 2.1. Since the binders were tested at 15ºC, the input energies selected from table 2.1 were the ones defined for 13ºC. This input energy can be input in equation 2.1, and using the parameters K1 and K2 from table 2.5, the N_{P20} value can be calculated for each project. The N_{P20} value is then compared with the traffic levels of table 2.2 to estimate the fatigue life. The results are shown in table 2.6.

TABLE 2.5 Time Sweep (N_{p20}) Binder Testing Results

Project	PG Grade	Stress [kPa]	G* [kPa]	Phase Angle [°]	Wi [kPa]	Np20 ($x10^3$)	K1	K2
9040-09-70	58 - 34	174	8607	50	8.506	232	1.889E+12	1.759
		123	8638	49	4.062	851		
9140-07-70	58 - 34	174	9621	49	7.514	257	1.488E+09	0.971
		140	8850	50	5.439	352		
1177-10-70	58 - 34	132	6323	54	6.981	135	1.031E+15	2.571
		110	6200	53	4.902	335		
6590-00-70	64 - 28	261	11477	51	14.438	93	3.478E+13	2.062
		196	12597	48	7.132	396		
1130-12-71	64 - 28	220	9542	52	12.510	68	2.042E+13	2.070
		154	10945	50	5.220	413		
3120-06-70	64 - 28	207	12370	47	7.918	316	1.337E+14	2.213
		166	11812	47	5.343	754		
4100-10-71	64 – 22	555	34465	40	17.992	113	1.597E+12	1.680
		390	36540	39	8.164	428		
1090-14-70	70 – 28	392	27645	46	12.467	50	4.062E+14	2.420
		274	34458	43	4.656	542		

TABLE 2.6 Allowable Traffic Volume (Based on N_{P20})

Project	PG Grade	Pavement Category	Wi [Pa]	N_{p20}	Allowable Traffic Volume (mill ESALs)
9040-09-70	58 - 34	Medium Highway	2500	1,991,845	0.3
9140-07-70	58 - 34	Medium Highway	2500	748,553	< 0.3
1177-10-70	58 - 34	Medium Highway	2500	1,893,019	0.3
6590-00-70	64 - 28	Minor Urban	5000	820,452	0.3
1130-12-71	64 - 28	Major Highway	500	52,867,385	10.0
3120-06-70	64 - 28	Minor Highway	6500	487,702	0.3
4100-10-71	64 – 22	Medium Urban	2000	4,545,425	1.0
1090-14-70	70 – 28	Major Highway	500	119,462,750	10.0

2.3.2 Stress Sweep and G*·sinδ

A surrogate fatigue test is currently under development between the University of Wisconsin Madison and the Federal Highway Administration. Experiments have shown that there is an inverse correlation between the stress at failure in the stress sweep test and the fatigue life of pavements. The results of the research are not conclusive yet. The stress sweep testing protocol was added to the present study as an update to the current trend.

The binders were RTFO aged and tested at 15ºC in a 8 mm DSR plate. The frequency of testing is the standard 10 Hz. The failure point was defined as the stress level required for 50% decrease in G*, compared with its initial value. Table 2.7 shows for each binder the stress required for 50% decrease in G*.

The results of the current fatigue specification parameter for the binders was also included to be compared with the new testing procedures. The last column of table 2.7 includes the G*sinδ, which is the current Superpave parameter for fatigue, for the PAV residue of the eight binders. These values were obtained from the WisDOT materials database.

TABLE 2.7 Stress Sweep Binder Testing Results and G*·sind **Values**

Project	PG Grade	G*ini [kPa]	Stress [kPa]	G*·sinδ [kPa]
9040-09-70	58 - 34	6360	344	2329
9140-07-70	58 - 34	7310	408	2419
1177-10-70	58 - 34	6530	375	2563
6590-00-70	64 - 28	12700	553	3244
1130-12-71	64 - 28	10500	479	2103
3120-06-70	64 - 28	10500	454	2391
4100-10-71	64 – 22	32300	1078	3299
1090-14-70	70 – 28	30300	1000	1226

2.4 Performance Data

The performance of the pavements was obtained from the WisDOT performance database. The data available includes every other year surveys of pavement distresses. Fatigue is a distress that usually appears in later stages of the pavement life. Due to the short duration of the present research project, advanced stages of fatigue cracking like alligator cracking were not observed. Only initial signs of fatigue cracking could be observed in the form of longitudinal cracking. The performance data available for the selected projects included winter 2004, summer 2004 and 2006. Table 2.8 shows the longitudinal cracking of each of the project sections for the mentioned survey periods. Each section has a length of approximately 1 mile.

As mentioned previously, all the projects were constructed in 2003. No signs of damage were found in the winter 2004 survey for any of the projects. The first signs of longitudinal cracking were found in the summer 2004 survey five of the projects (1177-10-70, 1130-12-71, 3120-06-70, 4100-10-71 and 1090-14-70). Two projects presented the first signs longitudinal cracking in the 2006 survey (9040-09-70 and 6590-00-70), while project 9140-07-70 did not show any sign of fatigue during the survey period. The kind of fatigue damage observed in all cases included longitudinal cracks with total length between less than 200 ft per station. One station is the survey unit and it is equivalent to 100 ft of pavement lane. The width of the cracks was less than one half of an inch.

TABLE 2.8 Longitudinal Cracking from Field Data

Project ID	Section ID	Winter 2004	Summer 2004	2006
9040-09-70	20090 & 160	-	-	1 to 100 feet per station / less than 1/2-inch in width
	20100, 110, 120, 130, 140, 150, 170, 180, 190, 200, 210 & 220	-	-	-
9140-07-70	87470, 480 & 490	-	-	-
	87500	NA	-	-
1177-10-70	68660	NA	-	1 to 100 feet per station / less than 1/2-inch in width
	68670, 680, 690, 700 & 710	-	-	-
	68720	NA	101 to 200 feet per station / band cracking	1 to 100 feet per station / less than 1/2-inch in width
6590-00-70	116410	-	-	-
	116420	-	-	1 to 100 feet per station / less than 1/2-inch in width
1130-12-71	54010	-	1 to 100 feet per station / less than 1/2-inch in width	1 to 100 feet per station / less than 1/2-inch in width
	54020	-	1 to 100 feet per station / less than 1/2-inch in width	NA
	54030; 52250 & 260	-	-	101 to 200 feet per station / less than 1/2-inch in width
	54040; 52270	-	101 to 200 feet per station / less than 1/2-inch in width	101 to 200 feet per station / less than 1/2-inch in width
	54050; 52290	N/A	101 to 200 feet per station / less than 1/2-inch in width	1 to 100 feet per station / less than 1/2-inch in width
	52280	-	1 to 100 feet per station / less than 1/2-inch in width	101 to 200 feet per station / less than 1/2-inch in width
3120-06-70	89150	N/A	101 to 200 feet per station / less than 1/2-inch in width	101 to 200 feet per station / less than 1/2-inch in width
	89160	N/A	1 to 100 feet per station / less than 1/2-inch in width	1 to 100 feet per station / less than 1/2-inch in width
	89170	N/A	-	1 to 100 feet per station / less than 1/2-inch in width
4100-10-71	126020 & 030; 126620 & 630	-	101 to 200 feet per station / less than 1/2-inch in width	101 to 200 feet per station / less than 1/2-inch in width
1090-14-70	57950; 135400	-	101 to 200 feet per station / band cracking	1 to 100 feet per station / less than 1/2-inch in width
	57960; 56390, 400 & 430; 135310 & 320	-	-	-
	57970, 980 & 990; 56410; 135330, 390, 410 & 420	-	-	1 to 100 feet per station / less than 1/2-inch in width
	56420	-	101 to 200 feet per station / less than 1/2-inch in width	-
	135300	NA	1 to 100 feet per station / less than 1/2-inch in width	1 to 100 feet per station / less than 1/2-inch in width

2.5 Relationship Between Pavement Performance and Binder Data

As discussed in the previous section, the field information on fatigue is very limited. Only initial signs of fatigue could be observed in the form of longitudinal cracking. It should be noted that the information available in the database does not allow to differentiate longitudinal cracking into joint cracking or fatigue (on wheel path) cracking. In the present section, the binder fatigue data will be compared with the initial signs of longitudinal cracking. Since the total fatigue life of the pavements is not available, the results are not expected to be conclusive.

In order to make a comparison, the information from table 2.8 has to be simplified. Each project has a certain number of sections. For a specific project, some sections showed fatigue damage before others. Table 2.9 shows the percentage of sections from each project that showed some sign of fatigue damage in each of the surveys.

By taking the design ESALs and growing rate from table 2.4, the accumulated ESALs can be estimated at the time of each of the surveys, as shown in table 2.10. Using the information from tables 2.9 and 2.10, the accumulated ESALs for the first signs of fatigue damage can be estimated for each project, as presented in table 2.11. These ESALs presented in table 2.11 are much lower than the allowable ESALs from table 2.6. The ESALs from table 2.6 represent the total fatigue life estimated from the binder Np20. The ESALs from table 2.11 are the ones accumulated when the first signs of fatigue damage were observed, which does not mean that the fatigue life has been reached.

TABLE 2.9 Percentage Project Sections With Fatigue Damage

Project ID	Winter 2004	Summer 2004	2006
9040-09-70	0%	0%	14%
9140-07-70	0%	0%	0%
1177-10-70	0%	14%	29%
6590-00-70	0%	0%	50%
1130-12-71	0%	70%	100%
3120-06-70	0%	67%	100%
4100-10-71	0%	100%	100%
1090-14-70	0%	22%	67%

TABLE 2.10 Estimated Accumulated ESALs

Project ID	Winter 2004	Summer 2004	2006
9040-09-70	60789	92519	259654
9140-07-70	52428	79441	219493
1177-10-70	67956	102870	283262
6590-00-70	27984	42487	118215
1130-12-71	668615	1013299	2801568
3120-06-70	27897	42265	116712
4100-10-71	167833	253913	697736
1090-14-70	598929	905341	2480377

TABLE 2.11 Cumulated ESALs at First Signs of Field Fatigue Damage

Project ID	Cumulated ESALs at First Signs of Field Fatigue Damage
9040-09-70	320838
9140-07-70	--
1177-10-70	118098
6590-00-70	140139
1130-12-71	1146768
3120-06-70	48889
4100-10-71	286622
1090-14-70	986099

A preliminary evaluation of the relevance of the binder N_{P20} values for estimating field fatigue life can be obtained by comparing the cumulated ESALs from table 2.11 with the binder N_{P20} values from table 2.6. This comparison is shown in figure 2.1. A logarithmic relationship can be obtained between the two variables.

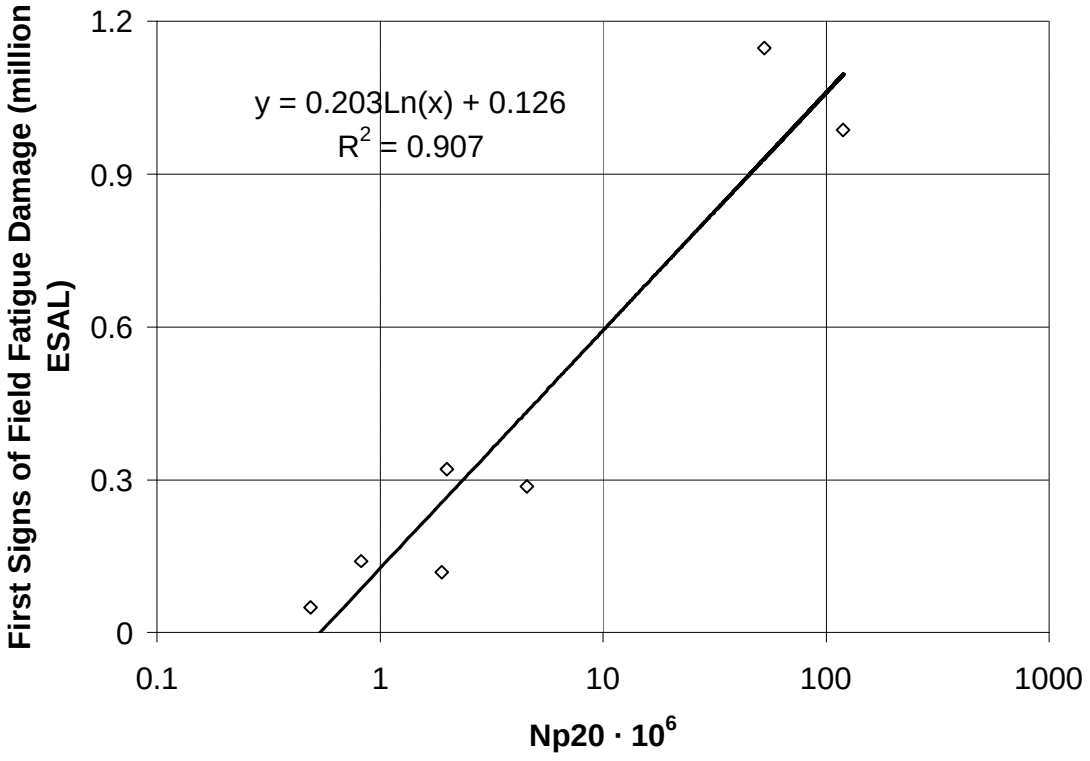

FIGURE 2.1 Binder N_{P20} Values v/s First Signs of Field Fatigue Damage

The results from both binder tests were compared in figure 2.2. No good correlation could be observed between the stress for 50% decrease in G* and N_{P20}. The stress sweep results were also compared with the field fatigue data, as presented in figure 2.3. No correlation could be observed between the stress required for 50% decrease in binder G* and the ESALs accumulated at the first signs of fatigue damage. The results, however, can not be considered conclusive due to the early and incomplete nature of the field data.

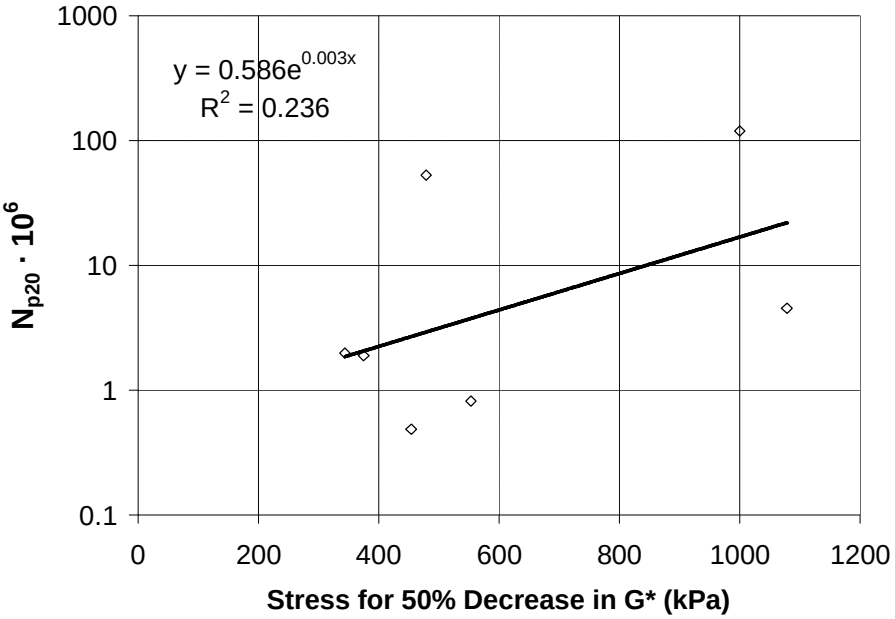

FIGURE 2.2 Stress Level to 50% decrease in G* v/s N_{P20}

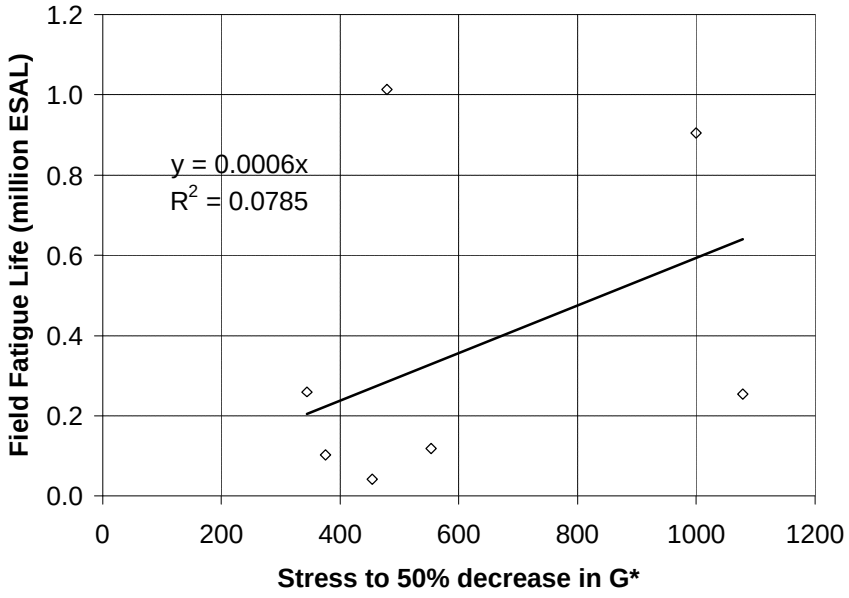

FIGURE 2.3 Stress Level to 50% decrease in G* v/s Field First Signs of Fatigue Damage

Finally, the relationship between N_{P20} and G*sinδ, and the relationship correlation between G*sinδ and the first signs of fatigue damage were studied. Figure 2.4 shows the N_{P20} values plot

against G*sinδ. No clear correlation could be found between the two values. Figure 2.5 presents the G*sinδ values against the first signs of field fatigue damage. Again, no clear correlation could be found between the two variables.

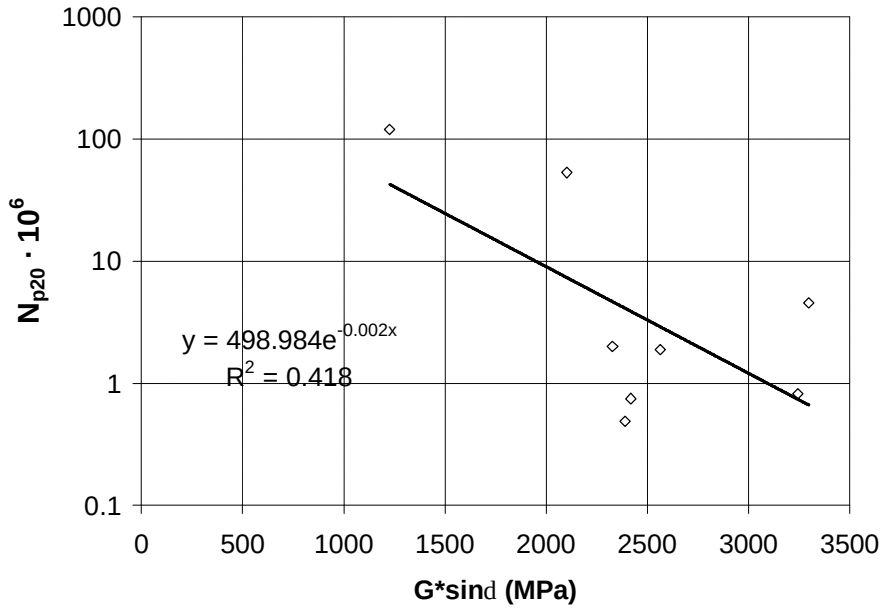

FIGURE 2.4 G*sind v/s N_{P20}

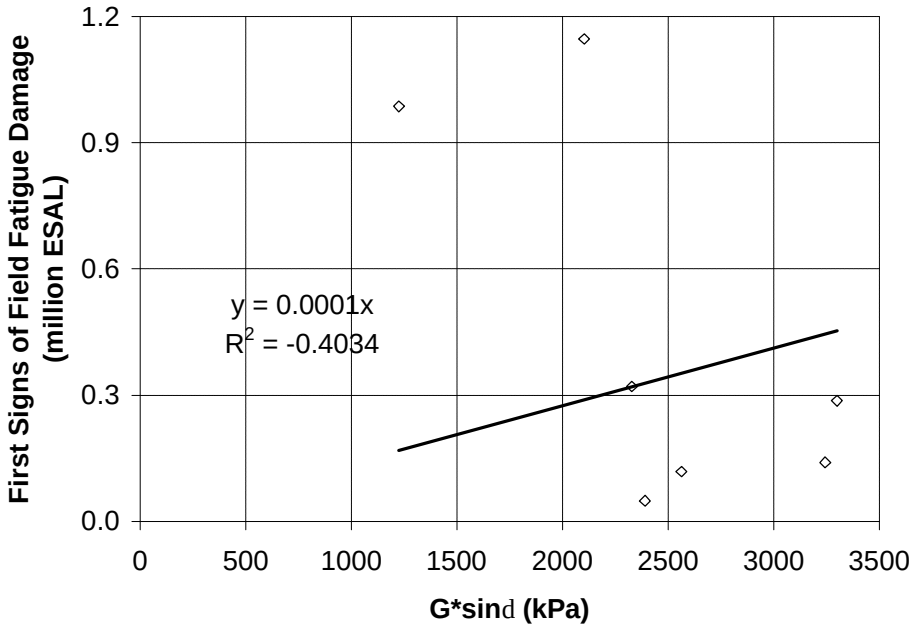

FIGURE 2.5 G*sind v/s Field First Signs of Fatigue Damage

2.6 Summary of Findings Fatigue Study

- G*sinδ does not correlate well with the first signs of pavement longitudinal cracking for the studied projects.
- G*sinδ did not correlate with N_{P20}, the new parameter proposed for binder fatigue characterization in the previous WisDOT report (Development of Guidelines for PG Binder Selection in Wisconsin, SPR# 0092-01-01)
- N_{P20} seem to correlate well with the first signs of pavement longitudinal cracking observed in the field during the first three years of service life of the selected projects.
- The surrogate binder fatigue test based on stress sweep, currently under consideration by the binder Expert Task Group did not correlate well to the first signs of field longitudinal cracking of the projects.
- Based on the above observations, it appears that N_{P20} is the best parameter, among the studied ones, for predicting the occurrence of longitudinal cracking.
- Performance data available in the WisDOT performance database included longitudinal cracking, but it did not differentiate between joint cracking and fatigue (at wheel path) cracking.

CHAPTER THREE: LOW TEMPERATURE CRACKING

3.1 Background

The present chapter focuses on the field validation of the low temperature cracking developed criterion in project 0092-01-01: Development of Guidelines for PG Binder Selection in Wisconsin [16]. The new procedure involves the explicit calculation of the binder cracking temperature for a specific cooling rate. The procedure involves testing binder with the Bending Beam Rheometer, the Direct Tension Tester (DTT) and the thermal contraction test or Tg test. The details of the testing procedure are described in detail on the literature [7, 16, 18].

For a specific binder, the BBR and DTT testing are carried out at three temperatures:

- Low temperature of PG grade +16ºC
- Low temperature of PG grade +10ºC
- Low temperature of PG grade +4ºC

The DTT testing is also carried out at different strain rates to include the effect of cooling rate on the cracking. A volumetric thermal shrinking test is carried out to determine the glass transition temperature Tg and the thermal contraction coefficients above Tg and below it. Figure 3.1 shows the flowchart of the calculation of the cracking temperature.

The validation will also include the PG criteria. The exact low temperature PG grade of the binders will be calculated and compared with the field performance of the project sections.

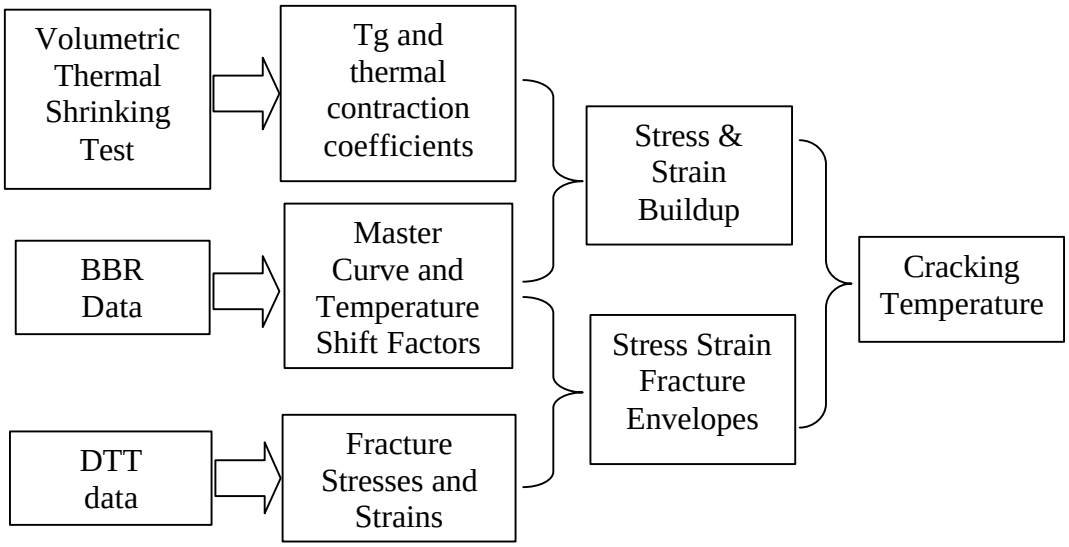

FIGURE 3.1 Flowchart for Determining Cracking Temperature

3.2 Selected Projects

Eight projects were selected for the validation of low temperature cracking criteria. The description of the projects is presented in table 3.1. The projects were the same eight projects selected for the validation of the fatigue criteria (seven projects using PMA binders and one with neat binder). The low temperature PG grade of the selected binders ranged from -34ºC to -22ºC. The type of base is also included in table 3.1. This information might be important to identify the possibility of reflective cracking form the underlying layer.

TABLE 3.1 Project and Sample Information

Project Name	DOT Project ID*	Binder	Polymer Modified	Type of Base	Construction Year
STH 17 Rhinelander Bypass	9040-09-70	58 - 34	YES	Pulverized HMA	2003
Charlotte Court - Clover Road (STH 64)	9140-07-70	58 - 34	YES	Pulverized HMA	2003
South County Line - CTH M (USH 51)	1177-10-70	58 - 34	YES	Existing AC	2003
Pine, Main & Mill Streets City of Weyauwega (STH 110)	6590-00-70	64 - 28	YES	Pulverized HMA	2003
De Pere-Green Bay-Lombardi Ave - IH 43 (USH 41)	1130-12-71	64 - 28	YES	Existing Concrete	2003
STH67 – Walworth County	3120-06-70	64 - 28	YES	N/A	2003
Calumet Ave., City of Manitowoc (USH 151)	4100-10-71	64 – 22	NO	Existing Concrete	2003
Airport Freeway (IH 894)	1090-14-70	70 – 28	YES	Rubblized Concrete	2003

* Refers to the project # assigned by the Wisconsin DOT

3.3 Binder Testing

RTFO samples of each of the binders were tested in the bending beam Rheometer. For each binder and each condition, three replicates were used. Table 3.2 shows the summary of the BBR testing results for the creep compliance after 60 seconds S(60) and the slope of relaxation m(60). The values shown are the average of the three measurements.

The Tg test was carried out using two samples per each binder. The summary of results from the test are shown in table 3.3. Tg refers to the glass transition temperature, α_l is the thermal coefficient above glass transition temperature and α_g is the thermal coefficient below glass transition temperature.

The DTT test was carried out for four of the projects only. The results from the DTT test showed very low repeatability for the fracture strain and fracture stress values. Table 3.4 shows

the averages and standard deviations of the DTT results. The number of samples tested per condition was between two and four. Due to the lack of repeatability, the information from the DTT test was proven to be not reliable for the determination of the cracking temperature, as it will be shown later. It was decided not to continue with the DTT testing for the rest of the binders. A different procedure was chosen to estimate the fracture stresses and strains. This will be discussed in a later section.

TABLE 3.2: Summary of BBR Testing Results

Project #	PG	Temperature	S(60)	m(60)
1090-14-70	70-28	-12 ºC	187	0.376
		-18 ºC	433	0.284
		-24 ºC	973	0.188
6590-00-70	64-28	-12 ºC	70	0.455
		-18 ºC	185	0.362
		-24 ºC	420	0.287
1177-10-70	58-34	-18 ºC	100	0.456
		-24 ºC	279	0.351
		-28 ºC	524	0.271
1130-12-71	64 - 28	-12	52.5	0.473
		-18	141.9	0.397
		-24	342.5	0.323
3120-06-70	64 - 28	-12	61.6	0.437
		-18	144.7	0.382
		-24	348.9	0.318
9040-09-70	58 - 34	-18	59.8	0.490
		-24	177.2	0.408
		-30	443.3	0.302
9140-07-70	58 - 34	-18	70.8	0.464
		-24	203.1	0.386
		-30	521.2	0.298
4100-01-71	64-22	-6 ºC	70	0.466
		-12 ºC	181	0.376
		-18 ºC	437	0.274

TABLE 3.3: Summary of Tg Testing Results

Project #	PG	Tg [ºC]	α_l [10^{-6}/ºC]	α_g [10^{-6}/ºC]
1130-12-71	64 - 28	-35	300	516
3120-06-70	64 - 28	-35	325	560
9040-09-70	58 - 34	-41	300	554
9140-07-70	58 - 34	-32	340	550
1090-14-70	70 - 28	-29	186	446
4100-10-71	64 - 22	-23	252	584
6590-00-70	64 - 28	-31	262	531
1177-10-70	58 - 34	-32	213	462

TABLE 3.4: Summary of DTT Testing Results

Project	Temp. ºC	Strain Rate	Fracture Strain %		Fracture Stress (MPa)	
			Average	SD	Average	SD
91400770 PG58-34	-18	3%	8.247	3.645	2.450	0.376
		10%	1.096	0.760	1.917	0.552
	-24	0.3%	2.102	1.417	2.673	1.538
		1%	1.484	1.250	2.790	1.598
		3%	0.648	0.213	2.485	0.474
		10%	0.312	0.023	1.630	0.170
	-30	0.3%	0.349	0.035	1.645	0.134
		1%	0.359	0.166	1.610	0.899
90400970 PG58-34	-18	10%	1.821	0.922	3.120	0.951
	-24	1%	2.315	0.675	4.233	0.447
		3%	0.787	0.419	3.173	1.191
		10%	0.911	0.231	5.163	0.962
	-30	0.3%	1.462	0.451	5.830	1.218
		1%	0.236	--	2.120	--
31200670 PG64-28	-18	1%	1.663	0.542	2.417	0.481
		3%	2.343	0.415	4.060	0.395
		10%	1.015	0.333	3.490	0.750
	-24	0.3%	0.841	0.351	2.365	0.629
11301271 PG64-28	-18	1%	7.027	2.178	3.233	0.206
		3%	2.669	0.625	4.257	0.467
		10%	2.291	0.566	5.570	0.806
	-24	0.3%	1.931	0.705	3.633	0.718
		1%	1.893	--	5.490	--

3.4 Performance Data

Low temperature damage is shown in the pavement as transverse cracking. Performance data was available from WisDOT performance database for winter 2004, summer 2004 and 2006. Table 3.5 shows the transverse cracking of each of the project sections for the mentioned survey periods. Each section has a length of approximately 1 mile.

The construction year for all eight projects was 2003. The winter 2004 survey did not show any sign of transverse cracking for any of the projects. In the summer 2004 survey four of the projects evidenced important amounts of transverse cracking (1130-12-71, 3120-06-70, 4100-10-71, 1090-14-70 and 1177-10-70). The reason why the summer 2004 survey showed damage for this projects and the winter 2004 survey did not is probably that the latter survey was carried out in the early winter, before the cracking happened. The rest of the projects did not show signs of low temperature cracking in the summer 2004 survey (9040-09-70, 9140-07-70 and 6590-00-70). In the summer 2006 survey all projects presented important amounts of transverse cracking, with the exception of projects 9040-09-70, 9140-07-70 and 6590-00-70 which did not show any sign or minimal transverse cracking.

TABLE 3.5 Transverse Cracking from Field Data

Project ID	Section ID	Winter 2004	Summer 2004	2006
9040-09-70 PG58-34	20090	-	-	1 to 5 cracks per station / less than 1/2-inch in width
	20100, 110, 120, 130, 140, 150, 160, 170,180, 190, 200, 210 & 220	-	-	-
9140-07-70 PG58-34	87470, 480, 490 & 500	-	-	-
	87500	NA	-	-
1177-10-70 PG58-34	68660 & 720	NA	6 to 10 cracks per station / less than 1/2-inch in width	6 to 10 cracks per station / less than 1/2-inch in width
	68670	-	-	1 to 5 cracks per station / less than 1/2-inch in width
	68670, 680, 690, 700 &710	-	-	-
6590-00-70	116410 & 420	-	-	-
1130-12-71 PG64-28	54010	-	1 to 5 cracks per station / less than 1/2-inch in width	1 to 5 cracks per station / less than 1/2-inch in width
	54020	-	1 to 5 cracks per station / less than 1/2-inch in width	NA
	54030; 52280	-	6 to 10 cracks per station / less than 1/2-inch in width	6 to 10 cracks per station / less than 1/2-inch in width
	54040; 52250 & 270	-	1 to 5 cracks per station / less than 1/2-inch in width	6 to 10 cracks per station / less than 1/2-inch in width
	54050	N/A	-	1 to 5 cracks per station / band cracking
	52260	-	1 to 5 cracks per station / less than 1/2-inch in width	1 to 5 cracks per station / less than 1/2-inch in width
	52290	NA	1 to 5 cracks per station / band cracking	-
3120-06-70 PG64-28	89150	N/A	1 to 5 cracks per station / band cracking	1 to 5 cracks per station / band cracking
	89160	N/A	-	1 to 5 cracks per station / less than 1/2-inch in width
	89170	N/A	-	-
4100-10-71 PG64-22	12020; 12630	-	1 to 5 cracks per station / less than 1/2-inch in width	6 to 10 cracks per station / less than 1/2-inch in width
	12030; 12620	-	6 to 10 cracks per station / less than 1/2-inch in width	6 to 10 cracks per station / less than 1/2-inch in width
1090-14-70 PG70-28	57950	-	6 to 10 cracks per station / band cracking	6 to 10 cracks per station / less than 1/2-inch in width
	57960; 56420 & 430; 135410	-	-	1 to 5 cracks per station / less than 1/2-inch in width
	57970, 980 & 990; 56390, 400 & 410; 135320 & 420	-	-	-
	135300	NA	1 to 5 cracks per station / less than 1/2-inch in width	1 to 5 cracks per station / less than 1/2-inch in width
	135310	-	1 to 5 cracks per station / less than 1/2-inch in width	-
	135330 & 400	-	-	1 to 5 cracks per station / band cracking
	135390	-	1 to 5 cracks per station / less than 1/2-inch in width	6 to 10 cracks per station / less than 1/2-inch in width

3.5 Cracking Temperature

As explained previously, the testing data from BBR, DTT and Tg tests are used to calculate the cracking temperature. The data from the BBR is used to construct a master curve of the creep compliance like the one shown in figure 3.2 for project 3120-06-70. From the shifting of the curves of the creep compliance at different temperatures, the temperature shift factor is obtained, as presented in figure 3.3 for the same binder.

In order to estimate the strain and stress buildup, the thermal coefficients and glass transition temperature have to be determined. The Tg test allows to calculate these three parameters. An example of the Tg test results is shown on figure 3.4 for project 3120-06-70. The last data set is obtained from the DTT testing. The fracture stresses and strain using several temperatures and speed rates are obtained, and the fracture envelopes are obtained like it is shown in figure 3.5 for the same project..

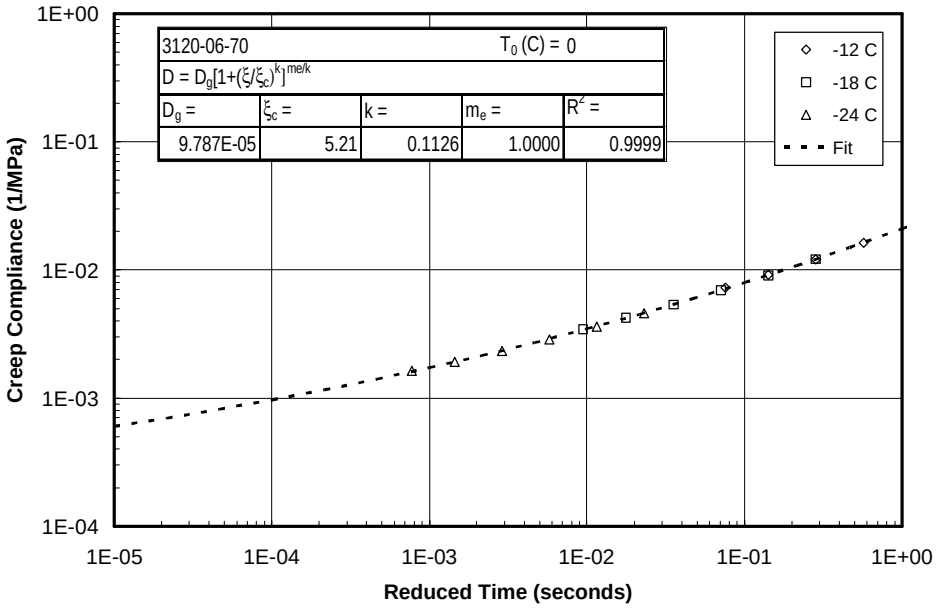

FIGURE 3.2 Creep Compliance Master Curve from BBR Data (3120-06-70)

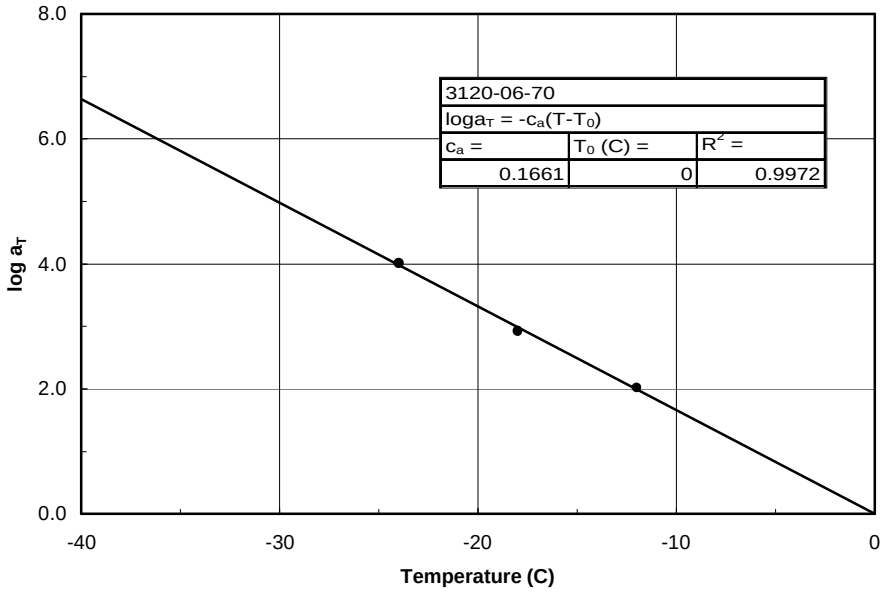

FIGURE 3.3 Temperature Shift Factor (3120-06-70)

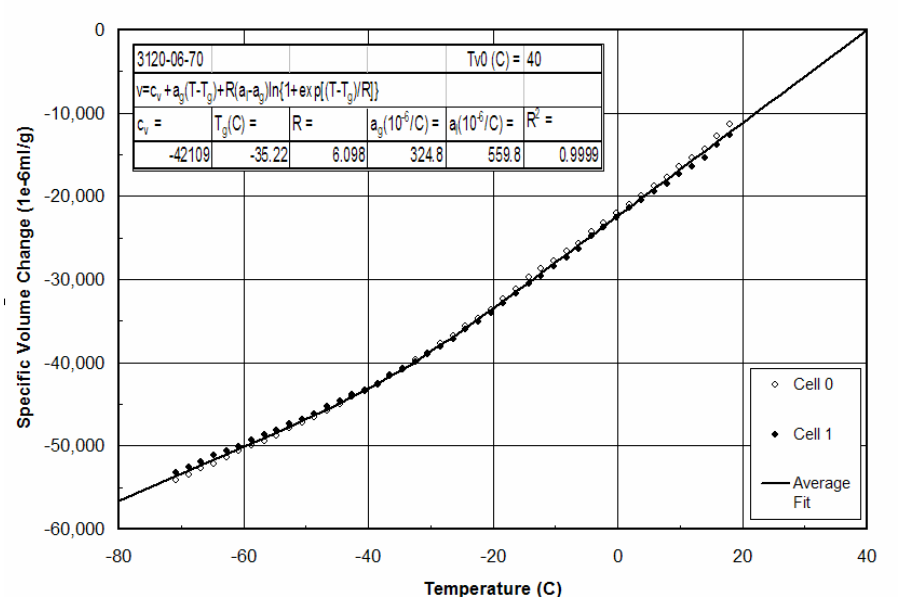

FIGURE 3.4 Thermal Contraction Curve (3120-06-70)

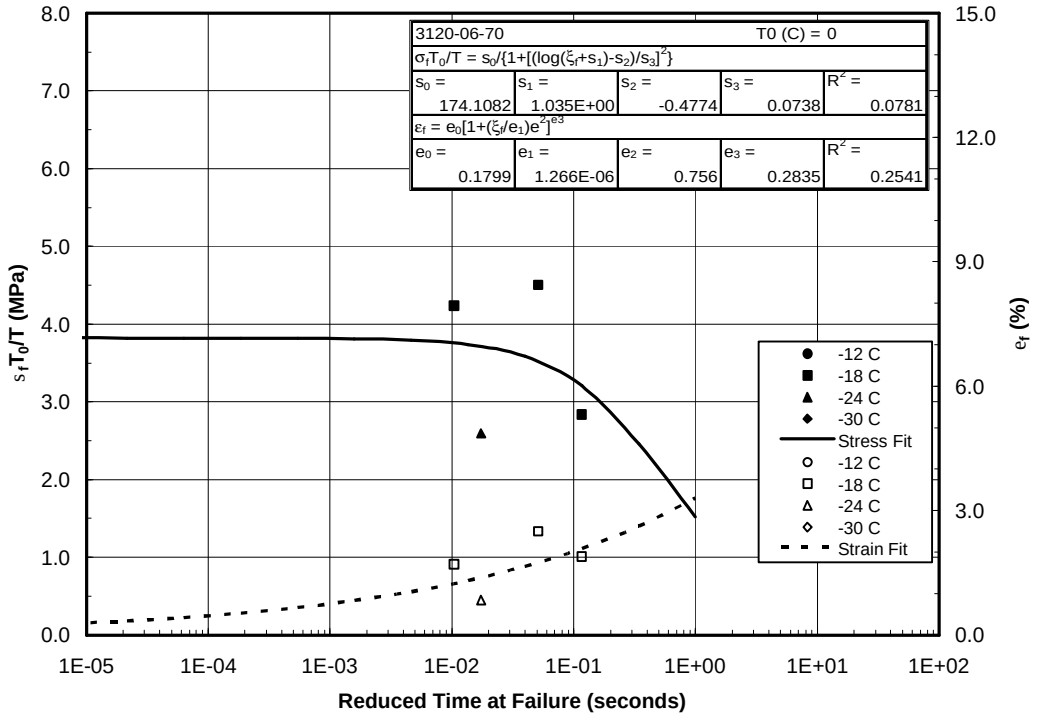

FIGURE 3.5 Fracture Curves (3120-06-70)

Finally, the cracking temperature is calculated. In previous research it was proposed that the cracking in the asphalt could happen either because the failure strain or the failure stress is reached (16, 18). The cracking temperature is then calculated using both criteria. The cracking temperature is the one where the thermal stress (or strain) curve intersects the failure stress (or strain) curve as shown in figures 3.6 and 3.7 for project 3120-06-70.

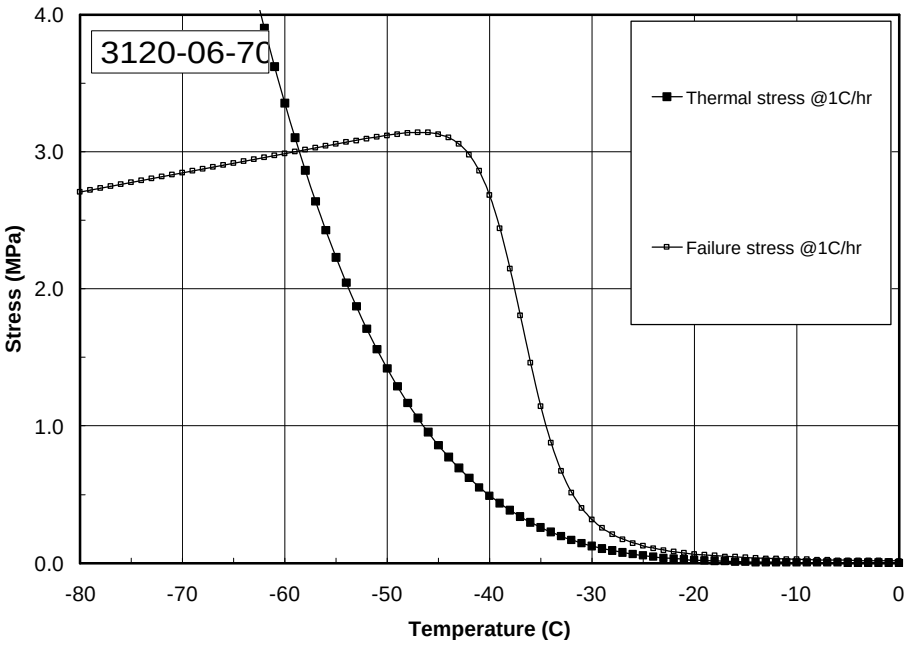

FIGURE 3.6 Cracking Temperature, Stress Criterion (3120-06-70)

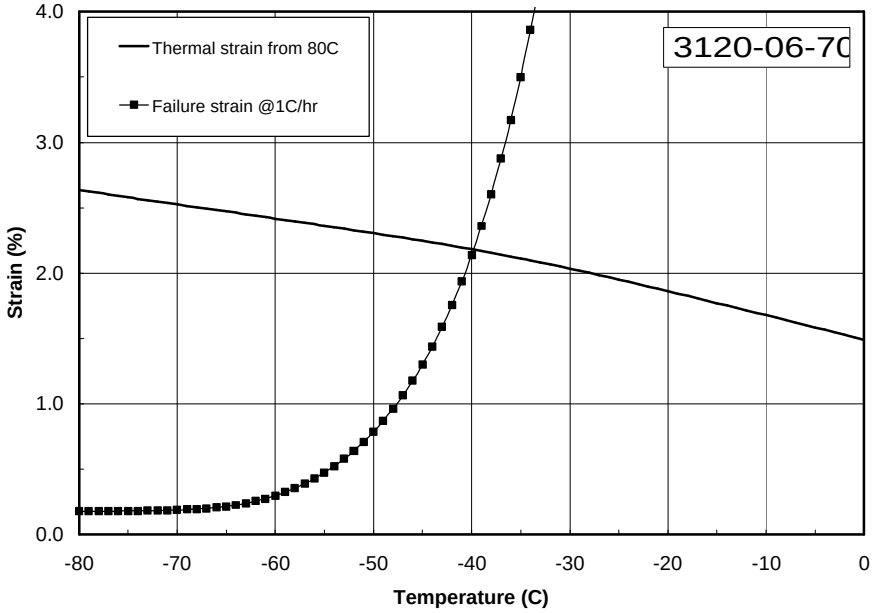

FIGURE 3.7 Cracking Temperature, Strain Criterion (3120-06-70)

During the testing of the binders, it was observed that the scatter of the results from DTT test was significant. This was mentioned before and it is shown by the high standard deviations in table 3.4. When the fracture stress and fracture strain curves were fitted to the DTT data, very low correlation coefficients were obtained. This can be evidenced by the R^2 values presented in figure 3.5. The lack of repeatability of DTT has been noticed before by many researchers. Because of the lack of reliability of the results, after testing four of the eight binders, it was decided to stop the DTT testing. To estimate the cracking temperature, it was decided to use average values for the failure strain and failure stress. The failure stress is the value of the y axis for the point where the thermal stress intersects the failure stress curve in figure 3.6. The failure stress is the corresponding point for figure 3.7. Table 3.6 shows the failure stress and strain for the four tested projects. The average values are shown in the last row. The cracking temperature was calculated as the temperature where the thermal strain/stress reaches the average failure strain/stress from table 3.6. Table 3.7 shows the results for the cracking temperature using both criteria. Cells that do not have any number mean that for that case, the thermal stress/strain did not reach the failure value. Previous research (19) showed that for the stress criterion to be more realistic, a scale factor of 18 needs to be used in the thermal stress. The factor is included in the calculations of table 3.7.

TABLE 3.6 Failure Strains and Stresses

Project	Failure Strain %	Failure Stress MPa
9040-09-70	2.24	3.62
9140-07-70	2.17	2.24
3120-06-70	2.18	3.01
1130-12-71	2.07	5.34*
AVERAGE	2.2	3.0

*Outlier, not considered in the calculation of the average

TABLE 3.7 Cracking Temperatures for Strain and Stress Criteria

Project	PG Grade	Cracking Temperature ºC	
		Strain Criterion	Stress Criterion
9040-09-70	58 - 34	-41	-35
9140-07-70	58 - 34	-45	-37
1177-10-70	58 - 34	NR *	-35
6590-00-70	64 - 28	-58	-31
1130-12-71	64 - 28	-58	-32
3120-06-70	64 - 28	-41	-32
4100-10-71	64 - 22	-47	-25
1090-14-70	70 - 28	NR *	-24

*Cracking temperature was not reached with the strain criteria

3.6 Weather Information

To complete the information needed for the analysis of the low temperature cracking criteria, the weather information for the field sites is needed. Using LTTP Bind program, the minimum yearly temperature and standard deviation were obtained for each of the project sites, as presented in table 3.8. The weather station used in each case was the closest one to each project.

TABLE 3.8 Minimum Temperatures per Project

Project ID	Weather Station ID	Minimum Yearly Temperature (ºC)	
		Average	Standard Deviation
9040-09-70	WI4829	-35.4	3
9140-07-70	WI0239	-33.5	3.3
1177-10-70	WI5516	-34.4	3.7
6590-00-70	WI8951	-29	3.6
1130-12-71	WI3269	-28.8	3.4
3120-06-70	WI4457	-26.4	3.7
4100-10-71	WI5017	-26.7	3.4
1090-14-70	WI5474	-25.6	3.7

3.7 Exact Critical Low Temperature based on Superpave Criteria

The Superpave specifications indicate a maximum value for S(60) of 300 MPa, and minimum value for m(60) of 0.300. From the BBR data, the temperatures at which the binders meet those specific values were calculated. It should be noticed that the Superpave specifications are based on PAV aged binder. The binders of this study are RTFO aged binders, so the critical temperature calculated in this section does not represent exactly the low temperature of the PG grade. The results are shown in Table 3.9.

TABLE 3.9: Critical Low Temperature (at Which S(60) = 300 Mpa)

Project ID	PG Grade	Temperature at which S(60) = 300 MPa
9040-09-70	PG58-34	-37
9140-07-70	PG58-34	-37
1177-10-70	PG58-34	-29
6590-00-70	PG64-28	-32
1130-12-71	PG64-28	-33
3120-06-70	PG64-28	-33
4100-10-71	PG64-22	-27
1090-14-70	PG70-28	-25

* Only the low temperature of the grade was adjusted. Temperature shown is that at which the S(60) = 300 Mpa.

In all cases, the determinant factor for the adjusted grade was the stiffness. If the m value was used instead of the stiffness for adjusting the grade, the low adjusted PG grade temperatures would have been lower. Table 3.9 shows that 5 of the binders showed an exact LT grade better than the specification PG grade. These results were expected because the BBR samples were prepared with RTFO material, which is more ductile and has a better low temperature resistance than PAV aged binder. RTFO aged binder was used instead of PAV because the validation included the field performance after one or two years of service. This means that short term

aging represents better the state of the binder inside the pavement of the selected projects when they failed. It is also important to note that for two binders the exact LT grade was higher than the specification PG grade.

3.8 Field and Binder Data Analysis

The field data from table 3.5 was summarized and the results expressed in average transverse cracks per mile, as shown in table 3.10. For each project, the number of cracks were calculated from the field data and then divided by the total project length. For the calculations, the sections classified in the "1 – 5 cracks per station" category were assumed to have three cracks per station. The sections in the "6 – 10 cracks per station category" were considered as having eight cracks per station.

TABLE 3.10 Transverse Cracks per Mile

Project ID	Transverse Cracks per Mile		
	Winter 2004	Summer 2004	2006
9040-09-70	0	0	11
9140-07-70	0	0	0
1177-10-70	0	121	143
6590-00-70	0	0	0
1130-12-71	0	195	259
3120-06-70	0	53	106
4100-10-71	0	290	422
1090-14-70	0	50	109

To obtain a correlation between the field performance and the binder criteria, three variables have to be taken into account at the same time: the field temperatures, low temperature criteria and pavement performance. Table 3.11 shows the summary of this information for all projects, gathered from previous tables. The third column of the table shows the field minimum yearly temperatures and standard deviations. The fourth column shows the temperature for which the

S(60) = 300 MPa is satisfied, with the reliability. Columns five and six show the critical cracking temperatures based on stress and strain criteria, with the corresponding reliability. Column seven shows the cracks per mile for each project obtained in the 2006 survey. The projects were ranked from the least amount of cracking to the highest amount of cracking.

The first important question is whether the calculation of the critical cracking temperature using the results of the BBR, Tg and DTT have any correlation to the critical temperature based on the Superpave criterion S(60) = 300 MPa. Figure 3.8 and 3.9 show the correlations for both criteria, stress and strain. It is observed in figure 3.8 that there is good correlation between the Superpave criterion and the cracking temperature from stress criteria. No correlation was found between the Superpave criterion and the critical cracking temperature from strain criterion.

TABLE 3.11 Summary of Low Temperature Information All Projects

Project ID	PG Grade	Field Air Temp (Std) ºC	Temp ºC for S(60)=300 MPa (Reliab %)	Critical Cracking Temp ºC (Reliab %)		Cracks Per Mile (2006)	Type of Base
				Stress Crit	Strain Crit		
9140-07-70	PG58-34	-33.5 (3.3)	-37 (86%)	-37 (86%)	-45 (>99%)	0	Pulverized HMA
6590-00-70	PG64-28	-29 (3.6)	-32 (80%)	-31 (71%)	-58 (>99%)	0	Pulverized HMA
9040-09-70	PG58-34	-35.4 (3)	-37 (70%)	-35 (45%)	-41 (97%)	11	Pulverized HMA
3120-06-70	PG64-28	-26.4 (3.7)	-33 (96%)	-32 (93%)	-41 (>99%)	106	N/A
1090-14-70	PG70-28	-25.6 (3.7)	-25 (44%)	-24 (33%)	NR (>99%)	109	Rubblized Concrete
1177-10-70	PG58-34	-34.4 (3.7)	-29 (7%)	-35 (56%)	NR (>99%)	143	Existing AC
1130-12-71	PG64-28	-28.8 (3.4)	-33 (89%)	-32 (83%)	-58 (>99%)	259	Existing Concrete
4100-10-71	PG64-22	-26.7 (3.4)	-27 (54%)	-25 (31%)	-47 (>99%)	422	Existing Concrete

The second question is whether the low temperature criteria are related to the field performance or not. One way to correlate the binder criteria to the field data is to build a graph between the reliability of each criteria and the field cracking. The reliability of each criterion indicates the certainty that low temperature cracking will not occur, based on that specific criterion. Figures 3.10 and 3.11 show the relationship between the cracks per mile and the reliabilities of the critical cracking temperatures based on Superpave criteria and stress cracking criteria. The strain criterion was not considered because it showed low correlation with the other two criteria and because the reliability in all cases but one was more than 99%, which is unrealistic. It can be seen in figures 3.10 and 3.11 that none of the criteria presented good correlation with the field data.

In table 3.11, the type of base for all projects is also shown. This information could be important because in overlay projects, the transverse cracking can be a combination of reflective cracking and thermal cracking. To eliminate the possibility of reflective cracking in the correlation, the projects that have existing concrete as a base (4100-10-71 and 1130-12-71) were excluded from the following analysis. Project 3120-06-70 was also excluded, because no data was found about the type of base. Figures 3.12 and 3.13 show the new correlations between the binder criteria and the field cracking without the mentioned projects. The relationship improved considerably for both criteria. However, it is the Superpave criterion (S(60) = 300MPa) the one that showed the best correlation with the field cracking (R = 0.93). The critical cracking temperature from the stress criterion showed an improved correlation, but not as good (R = 0.31). The strain criterion was not considered for the reasons explained earlier.

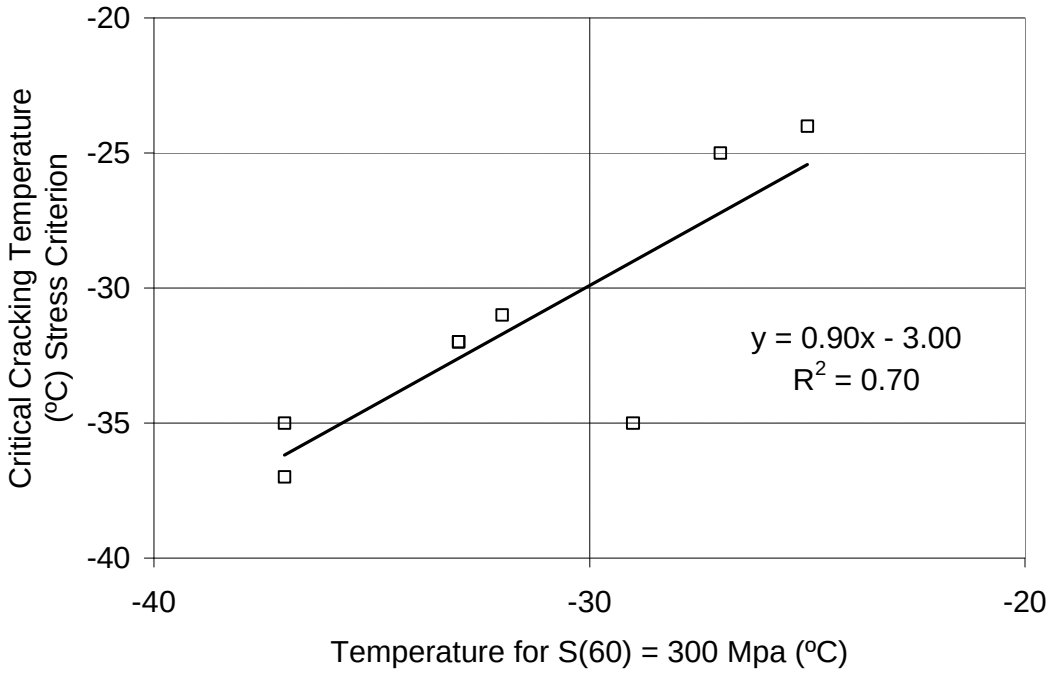

FIGURE 3.8 Correlation Between Critical Cracking Temperature - Stress Criterion and Temperature for S(60) = 300 MPa

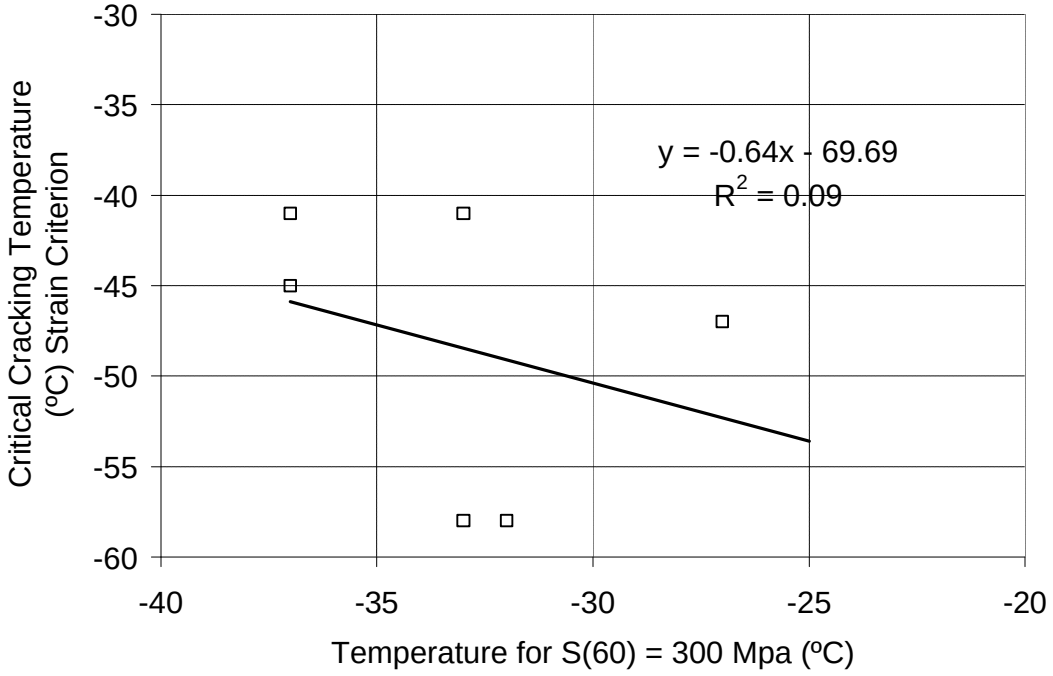

FIGURE 3.9 Correlation Between Critical Cracking Temperature - Strain Criterion and Temperature for S(60) = 300 MPa

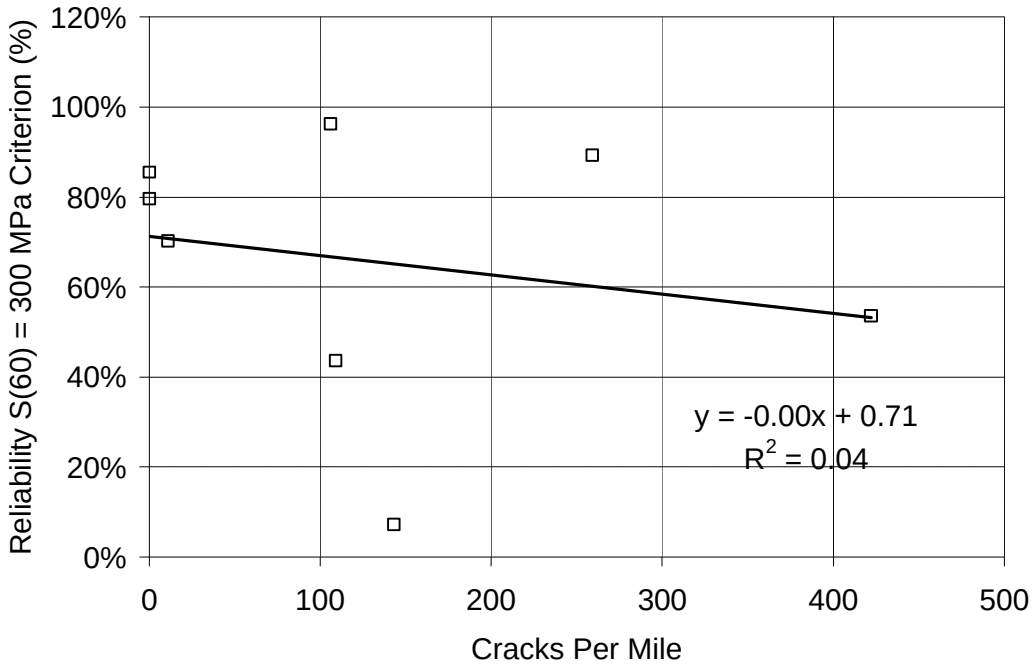

FIGURE 3.10 Correlation Between Reliability of Temperature for S(60) = 300 MPa Criterion and Field Cracking

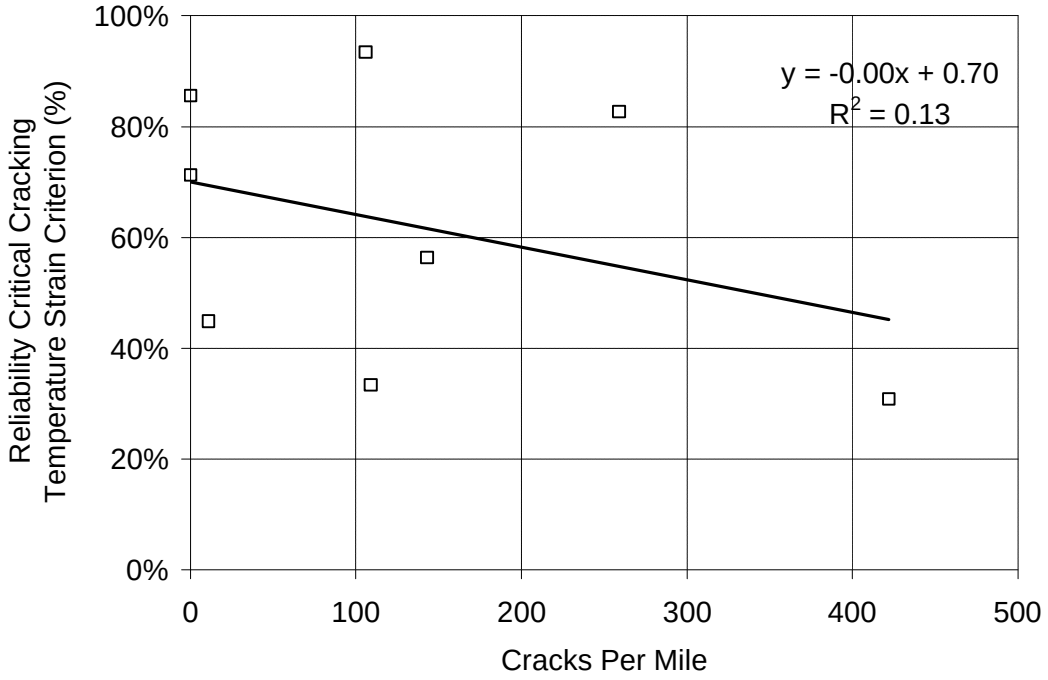

FIGURE 3.11 Correlation Between Reliability of Critical Cracking Temperature – Stress Criterion and Field Cracking

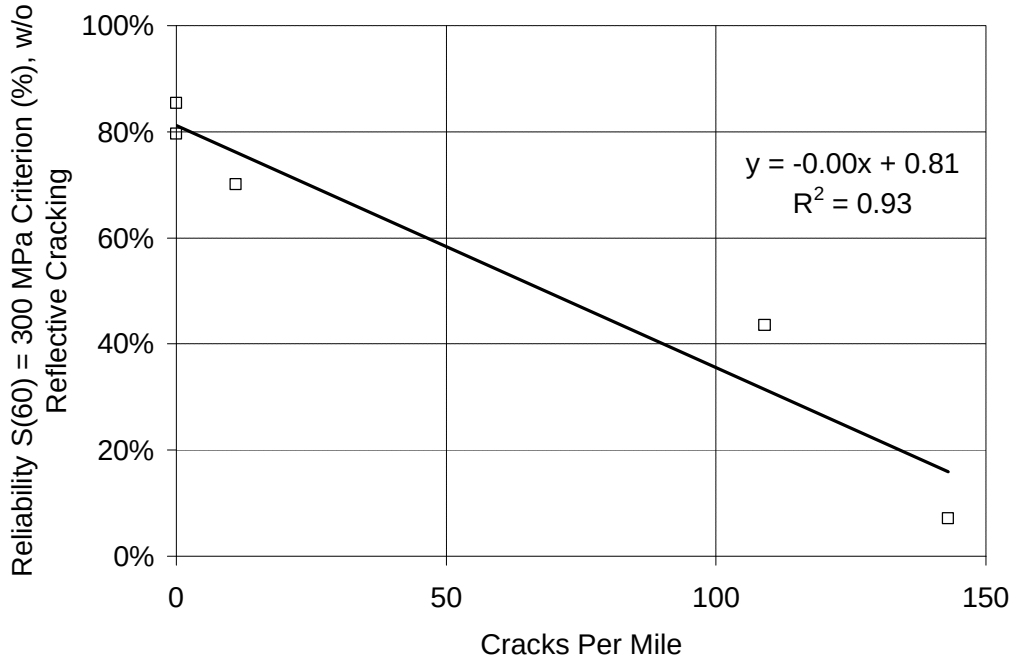

FIGURE 3.12 Correlation Between Reliability of Temperature for S(60) = 300 MPa Criterion and Field Cracking, Excluding Reflective Cracking

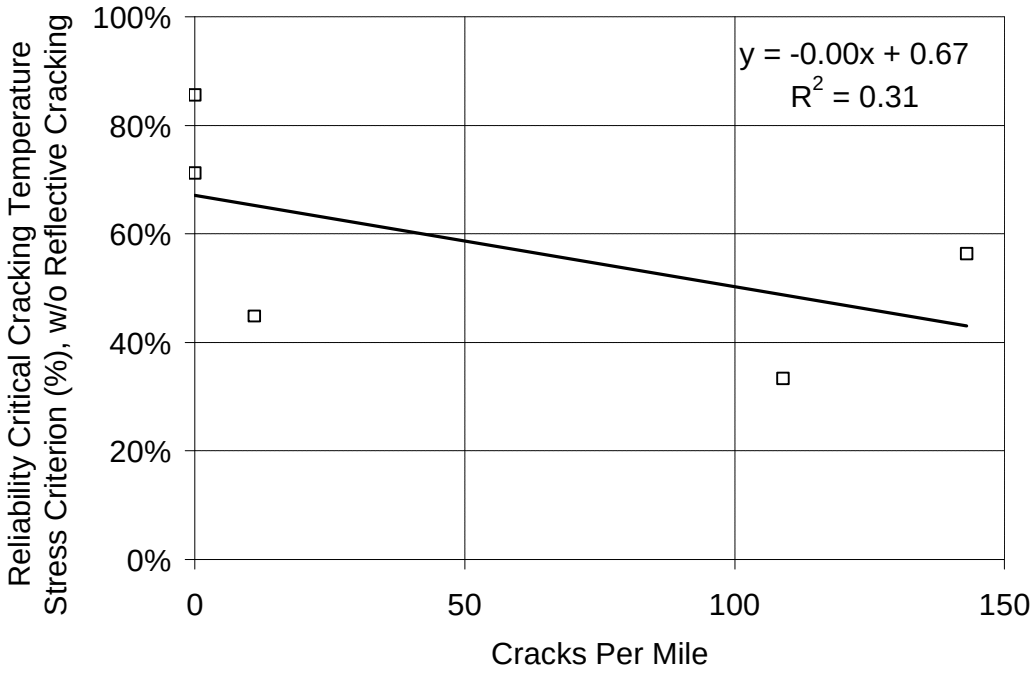

FIGURE 3.13 Correlation Between Reliability of Critical Cracking Temperature – Stress Criterion and Field Cracking, Excluding Reflective Cracking

3.9 Summary of Findings Low Temperature Study

- Due to the difficulty of obtaining the repeatability needed from the DTT test, correlations were sought between BBR and DTT results. Based on the limited data, critical cracking temperatures based on the stress criteria correlates somewhat (R=70%) with critical temperature based on S(60) from BBR. Therefore, one could ignore measuring stress at failure. However, no correlation with critical temperature using strain criteria was found. Therefore, if strain is required to predict cracking, the DTT has to be used.
- To look at correlation with field performance, distinction between reflective & purely thermal cracking had to be made. For thermal cracking it is clear that reliability of S(60) (probability of critical cracking temperature based on S(60) to be lower than minimal air temperature) gave the best correlation. At a reliability above 70%, there appears to be no cracking during the first three years
- None of the other parameters, including DTT and m(60), showed good correlation with thermal cracking on pavements.

CHAPTER FOUR: RUTTING

4.1 Background

The new proposed binder specifications for rutting are based on creep and recovery testing using the Dynamic Shear Rheometer. Original and RTFO aged binder samples are tested at 58ºC, which was chosen as the standard HT PG grade for Wisconsin. The binders are tested for 100 cycles of creep and recovery with 25 Pa of shear stress. The viscous component of the creep stiffness G_v is calculated for the binder, based on the Burgers model. The details of the testing procedure and analysis can be found in the literature (7, 16, 20). A minimum G_v value is specified for each traffic level. Two different values of traffic speed are recognized, in order to take into account the low speed movements of the urban areas, which are more critical to rutting. The proposed rutting specifications are presented on table 4.1.

TABLE 4.1 Proposed Rutting Specifications

Purpose	Testing Rate	Testing Stress	Testing Temperature	Traffic Level (Millions ESALs)					
				0 - 0.3	0.3 - 1	1 - 3	3 -10	10 - 30	> 30
Test on Original Binder									
Traffic Speed	Load / unload	Creep Stress		Minimum G_v at loading time (MPa)					
60 mph	0.01/ 0.09 s	25 Pa	58°C	1.0	5.0	15.0	50.0	150.0	> 200
15 mph	0.04/ 0.36 s	25 Pa	58°C	4.0	20.0	60.0	200.0	600.0	> 800
Test on RTFO Aged Binder									
Rutting Resistance	Load / unload	Creep Stress		Minimum G_v at loading time (MPa)					
60 mph	0.01/ 0.09 s	25 Pa	58°C	1.25	6.0	18.0	60.0	180.0	> 250
15 mph	0.04/ 0.36 s	25 Pa	58°C	5.0	24.0	72.0	240.0	720.0	> 1000

4.2 Selected Projects

The projects selected for the field validation of the rutting specifications are presented in table 4.2. Three different high temperature PG grades were considered: 58C, 64C and 70C, including four PMA binders and two neat binders. The project traffic data, design life and design speed is presented in table 4.3. No traffic information was found for project 7132-04-61. The design ESALs value shown in the table for this project was estimated based on the material information for the project, which indicated that an E-1 mixture was used for the surface layer.

TABLE 4.2 Project and Sample Information

Project Name	DOT Project ID*	Binder	Polymer Modified	Construction Year
STH 17 Rhinelander Bypass	9040-09-70	58 - 34	YES	2003
Charlotte Court - Clover Road (STH 64)	9140-07-70	58 - 34	YES	2003
I – 94 Baldwin	1020-01-74	70 - 28	YES	2003
STH 95 Arcadia - Fountain City	7132-04-61	58 - 28	NO	2004
USH 51, Iron County	1170-13-70	64 - 34	YES	2005
Whitewater Bypass (USH 12)	1080-00-72	58-28	NO	2003

* Refers to the project # assigned by the Wisconsin DOT

TABLE 4.3 Traffic Data and Design Life

Project ID	Design ESALs	Growing Rate (Linear)	Design Life (years)	Design Speed (mph)
9040-09-70	2029400	2.4%	20	60
9140-07-70	1511101	1.5%	20	55
1020-01-74	42350300	2.5%	20	70
7132-04-61	800000	1.5%	20	55
1170-13-70	2284900	1.5%	20	45
1080-00-72	1752000	1.5%	20	70

4.3 Binder Testing

Original (non-aged) and RTFO (short term aging) aged binders were tested. The value of G_v was determined for each of the binders. The testing temperature was 58ºC and the testing stress 25 Pa. The stress-controlled rheometer is programmed to run a repeated creep test of a total of 100 cycles of 1 second loading and 9 seconds unloading. Table 4.4 shows the G_v values for the testing conditions in its third and fourth column. As explained in a previous report (16), the G_v values need to be adjusted according to the expected traffic speed. For highways, the G_v need to be divided by 0.01. For urban roads G_v, needs to be divided by 0.04. The four columns on the right side of table 4.4 show the G_v values for highway and urban applications.

The binders were also tested using the Multiple Stress Creep and Recovery test MSCR. This procedure considers testing the RTFO residue of the binder at the high temperature of the PG grade using the DSR. Ten cycles of 1 second creep and 9 seconds recovery are applied to the binder sample at 100 Pa. Immediately after that, ten more cycles are applied at 3200 Pa. The results of the test are the percentage recovery $\%\varepsilon_r$ and the non recoverable compliance Jnr. The details of the testing procedure are described in the literature (21). Table 4.5 shows the results of the MSCR test for the binders considered in this section. To allow further comparison with the current procedure, the $G^*/\sin\delta$ values were also included in the table. The latter values were taken from the WisDOT materials database.

TABLE 4.4 Binder G_v Values

Project ID	Binder	G_v (kPa)					
		1 s – 9 s		0.04 s – 0.36 s (Urban)		0.01 s – 0.09 s (Highway)	
		Original	RTFO	Original	RTFO	Original	RTFO
9040-09-70	58 - 34	362	1273	9062	31815	36247	127261
9140-07-70	58 - 34	224	725	5603	18133	22412	72532
1020-01-74	70 - 28	2408	9075	60198	226872	240793	907489
7132-04-61	58 - 28	145	1484	3615	37096	14459	148385
1170-13-70	64 - 34	1004	6249	25112	156224	100449	624897
1080-00-72	58 - 28	168	393	4196	9828	16786	39310

TABLE 4.5 Binder MSCR and G*/sind **Test Results**

Project ID	Binder	MSCR $\%\varepsilon_r$		MSCR J_{nr}		G*/sinδ (kPa	
		100 Pa	3200 Pa	100 Pa	3200 Pa	Original	RTFO
9040-09-70	58 - 34	50%	37%	0.05	0.06	1.25	3.14
9140-07-70	58 - 34	45%	31%	0.05	0.07	1.15	2.92
1020-01-74	70 - 28	47%	33%	0.09	0.11	1.18	2.44
7132-04-61	58 - 28	2.6%	%0	0.19	0.20	1.28	N/A
1170-13-70	64 - 34	61%	53%	0.07	0.08	1.13	2.9
1080-00-72	58 - 28	1.4%	0%	0.22	0.24	1.19	2.27

4.4 Field and Binder Data Analysis

Unfortunately , up to the present, no field rutting has been observed in any of the projects. The survey data gathered for the last two years showed no signs of permanent deformation in any of the projects, according WisDOT performance database. Because of this, the field validation achieved to this point is limited and can not be conclusive. Some preliminary analysis will be carried out as follows.

The speed category of every project is shown in column three of table 4.6. Five of the projects were in the 55 mph – 70 mph category. These were fit into the 60 mph category. One of the projects had a design speed of 45 mph (1170-13-70). To be conservative, the speed category for this project was chosen as 15 mph, instead of 60 mph. Columns four and five of table 4.6 show the G_v values corresponding to the speed category, taken from table 4.4. Then, the allowable ESALs are calculated from table 4.1, by fitting the G_v value with the ESALs category, for the corresponding speed. The allowable ESALs for each project are shown in column 6 of table 2.6.

TABLE 4.6 Allowable Traffic Volume (Based on G_v)

Project	PG Grade	Speed Category (mph)	Gv [kPa]		Allowable Traffic Volume (mill ESALs)	Estimate Traffic up to 2006 (mill ESALs)
			Original	RTFO		
9040-09-70	58 - 34	60	36247	127261	3.0	0.32
9140-07-70	58 - 34	60	22412	72532	3.0	0.26
1020-01-74	70 - 28	60	240793	907489	30	6.7
7132-04-61	58 - 28	60	14459	148385	1.0	0.13
1170-13-70	64 - 34	15	25112	156224	1.0	0.39
1080-00-72	58 - 28	60	16786	39310	3.0	0.30

Finally, the estimated accumulated traffic up to 2006 can be estimated for each project using the design ESALs and the growth rates (column seven of table 4.6). By comparing the allowable ESALs with the estimated traffic up to date for each project (columns six and seven of table 4.6), it can be seen that for none of the projects the allowable traffic volume has been reached. So, according to the predictions based on G_v, the allowable ESALs have not been reached, which agrees with field data where no rutting damage was found.

The results of the binder tests were also compared with each other. Figure 4.1 shows the plot of G*/sinδ against G_v measured values for the RTFO residue. No clear correlation was found between the two parameters.

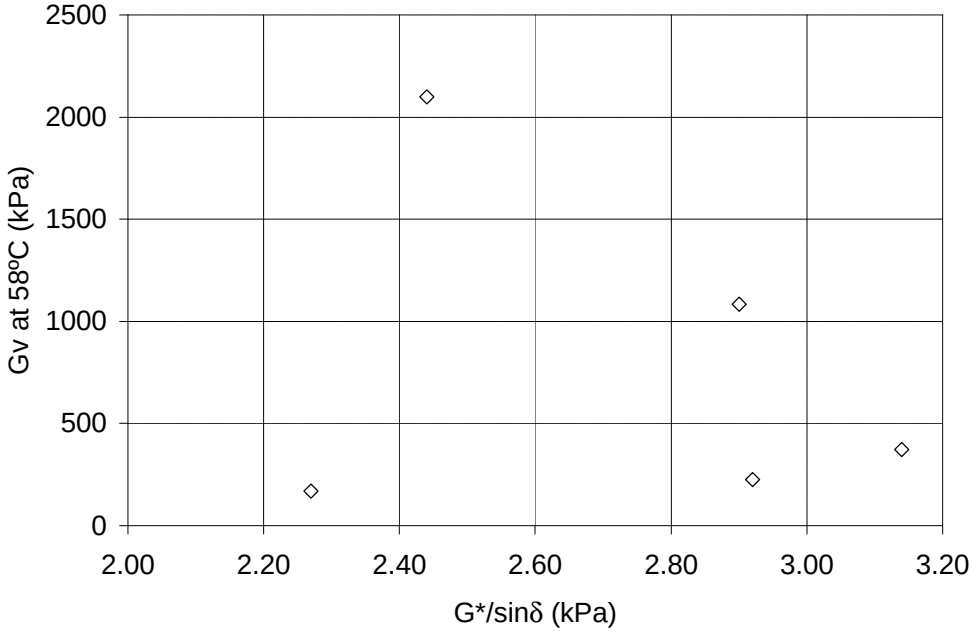

FIGURE 4.1 G*/sind v/s G_v (at 58ºC), RTFO Residue

The correlation between G_v and Jnr was also found to be not very good, as shown in figure 4.2. When the G*/sinδ values were compared with Jnr, a trend was found. Figure 4.3 shows how there is an inverse correlation between the two parameters. The correlation was not as good between $\%\varepsilon_r$ from MSCR and G*/sinδ, as shown in figure 4.4. The relationship between the binder parameters considered in this section is as expected. MSCR and G*/sinδ are carried out at the high temperature of the PG grade, so its result are better correlated. G_v on the other side, was measured at 58ºC for all the binders. Since in the group of binders there were binders of high

temperature of the PG grade equal to 58ºC, 64ºC and 70ºC, it is expected that the values measured at 58ºC for G_v do not correlate with the rest of the parameters.

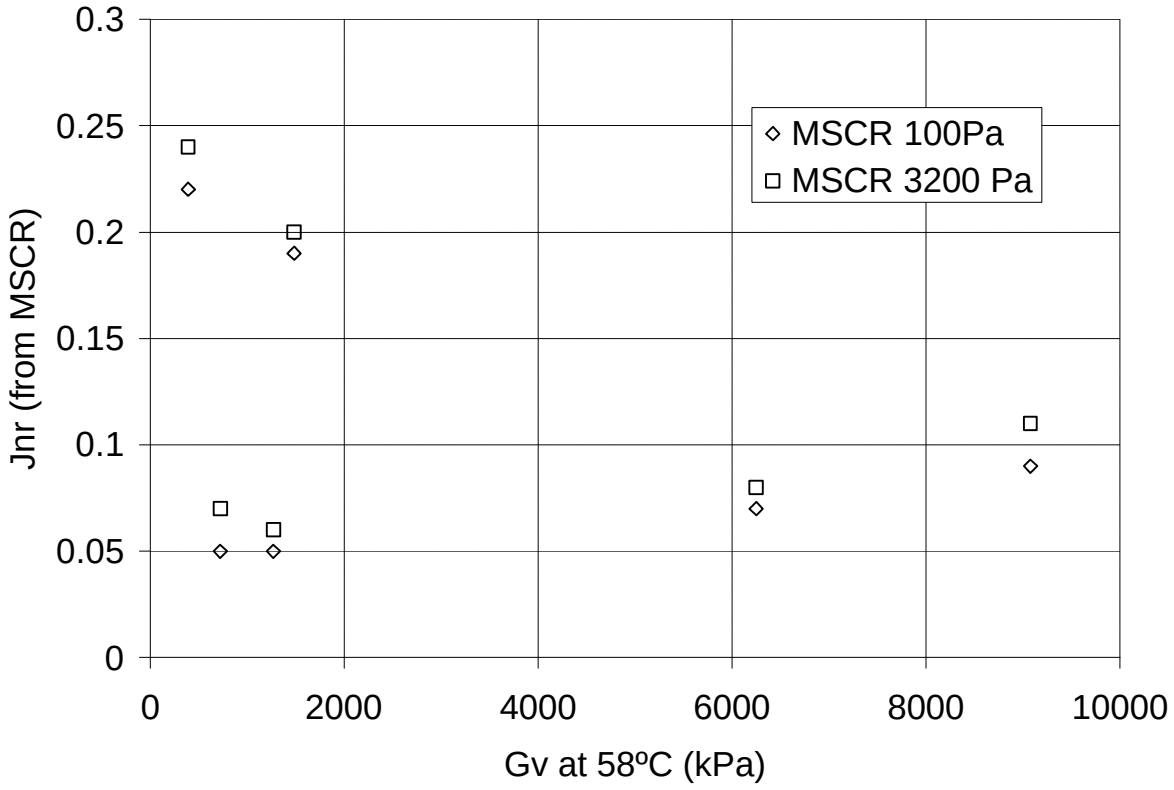

FIGURE 4.2 Gv (at 58ºC) v/s Jnr, RTFO Residue

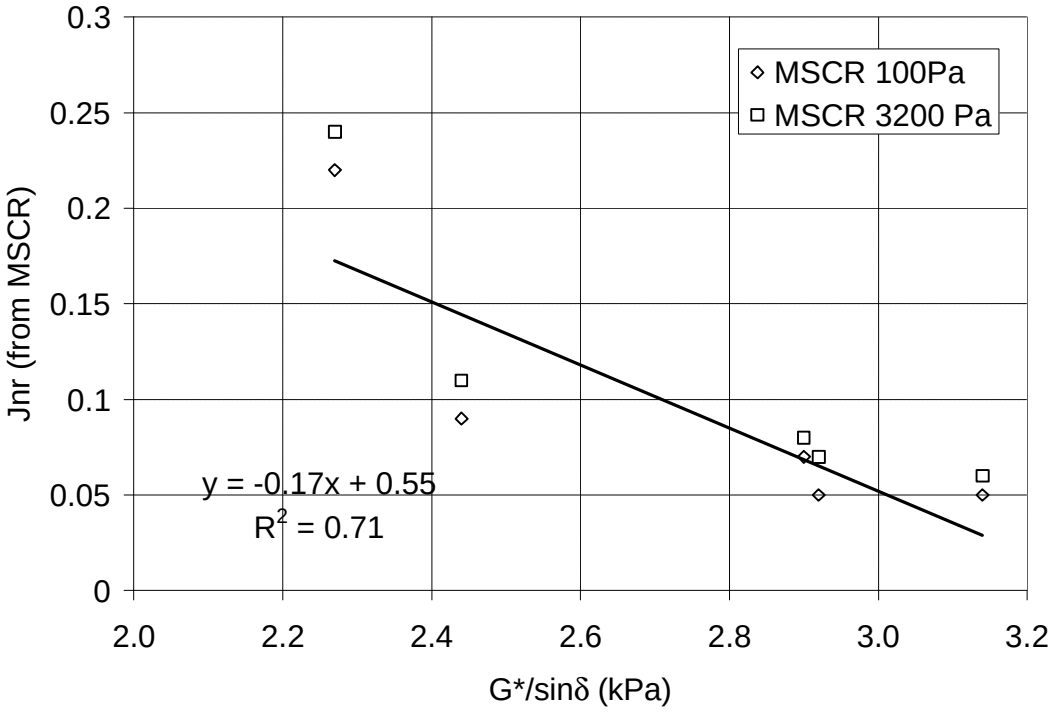

FIGURE 4.3 G*/sind v/s Jnr, RTFO Residue

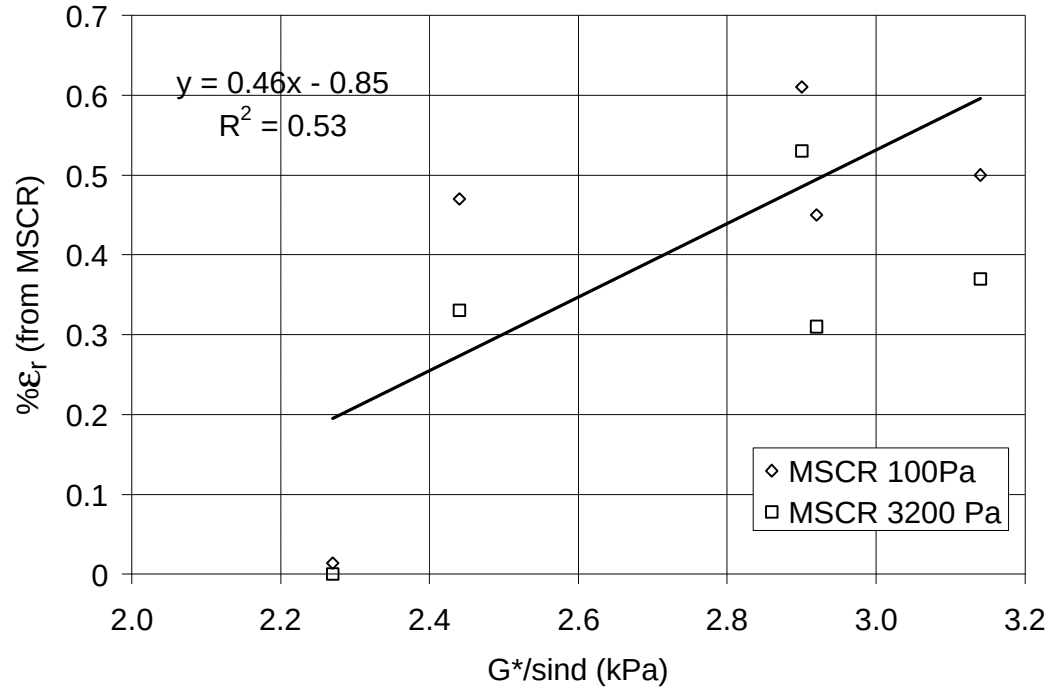

FIGURE 4.4 G*/sind v/s %e_r , RTFO Residue

4.5 Summary of Findings Rutting Study

- Up to the last field survey, there was no rutting observed in the field for the selected projects
- Elastic recovery (%ε_r) measured using the MSCR test was compared with G*/sinδ. There appear to be some correlation between the two parameters. However, the %ε_r can clearly differentiate between modified and unmodified binders.
- WisDOT is currently using Elastic Recovery ER measured by the ductilimeter, to identify PMA binders. The current data showed that using the DSR with the MSCR protocol, the same purpose can be achieved with a much simpler test and without the need for ductilimeter.
- G_v, which is the parameter recommended in the previous WisDOT study (Development of Guidelines for PG Binder Selection in Wisconsin, SPR# 0092-01-01), did not correlate with MSCR results. It is, however, important to realize that G_v was measured at 58ºC, while MSCR is done at the high temperature of the PG grade.
- The research team maintains the validity of G_v, based on the presented data. The pavement performance information indicated that no rutting data was observed yet. The estimated traffic in all the sections up to 2006 was below what was calculated as allowable based on G_v. This means that according to the predictions based on G_v, no field rutting damage was expected up to date, and that agrees with the field observations.

CHAPTER FIVE: RECOMMENDATIONS

The present project consisted on the field validation of the asphalt binder recommendations developed in a previous WisDOT study (Development of Guidelines for PG Binder Selection in Wisconsin, SPR# 0092-01-01). Four main areas were looked at: mixing and compaction temperatures, fatigue cracking, low temperature cracking and rutting damage. The following recommendations are made based on the findings listed on the previous chapters.

- Mixing and Compaction: It is clear from this study, that compaction temperatures currently used in the field could be reduced without reduction in density. This is observed for modified and unmodified binders. It is recommended that WisDOT, in collaboration with contractors, spend an effort to verify the results of this study and develop guidelines to target the optimum zone construction temperatures. In laboratory mix design procedures, temperatures at which viscosities equal to 50 Pa·s should be used. This will encourage contractors to realize that the high temperatures used today in the field are not necessary.
- Fatigue: Although the parameter proposed in the previous study (N_{P20}) showed good correlation with longitudinal cracking, it is premature to make specific recommendations. The reason being the existing database does not allow differentiating joint cracks and wheel path cracks.
- Thermal Cracking: Field data correlated extremely well with BBR S(60) measurements. There appears to be no need to change the existing practice of the DOT. The limited data collected for DTT can not be used to justify the need for it.

- Rutting: The section that followed during the duration of the project did have not shown any sign of rutting damage yet. MSCR $\%\varepsilon_r$ and $G^*/\sin\delta$ give a fair correlation. With the limited data it is not clear whether we need to change $G^*/\sin\delta$. However, it is clear that the MSCR test can be used to differentiate between modified and unmodified binders. The issue of replacing $G^*/\sin\delta$ with G_v and MSCR test can not be concluded due to the lack of rutting on the pavement sections.
- Database: On electronic copy of performance and materials database has been developed and delivered for the project. It is highly recommended that the database be maintained and updated for future changes in asphalt grading in Wisconsin.

REFERENCES

1. Roberts F., P. Kandhal, E Ray Brown, D. Lee and T. Kennedy. Hot Mix Asphalt Materials, Mixture Design and Construction. NAPA Research and Educational Foundation, 1996.

2. R. J. Cominsky, G. A. Huber, T. W. Kennedy, and R. M. Anderson. The Superpave Mix Design Manual for New Construction and Overlays. Strategic Highway Research Program, SHRP-A-407, 1994.

3. Faheem, A., H. Bahia, and H. Ajideh. Estimating Results of a Proposed Simple Performance Test for Hot Mix Asphalt from Superpave Gyratory Compactor. In *Transportation Research Record: Journal of the Transportation Research Board*, No 1929, TRB, National Research Council, Washington, D.C., 2005, pp 104-113.

4. Khatri, A., H. Bahia and D. Hanson. Mixing and Compaction Temperatures for Modified Binders using the Superpave Gyratory Compactor. *Journal of the Association of Asphalt Paving Technologists,* Vol. 70, 2001, pp. 368-395.

5. Cho, D.W., H.U. Bahia and N. Kamel. Critical Evaluation of Use of the Procedure of Superpave Volumetric Mixture Design for Modified Binders. In *Transportation Research Record: Journal of the Transportation Research Board*, No 1929, TRB, National Research Council, Washington, D.C., 2005, pp 114 – 125.

6. DeSombre, R., D. E. Newcomb, B. Chadbourn, and V. Voller. Parameters to Define the Laboratory Compaction Temperature Range of Hot Mix Asphalt. *Journal of the Association of Asphalt Paving Technologists.* Volume 67, Boston, Massachusetts. 1998.

7. Bahia, H.U., D.I. Hanson, M. Zeng, H. Zhai, M.A. Khatri and R.M. Anderson. Characterization of Modified Asphalt Binders in Superpave Mix Design. Publication NCHRP 459, National Academy Press, Washington, D.C., 2001.

8. Y. Yildrim, M. Solaimanian, and T. Kennedy. Mixing and Compaction Temperatures for Superpave Mixes. *Journal of the Association of Asphalt Paving Technologists.* Vol. 69. Reno, Nevada. 2000.

9. Kamel. N., Bahia, H., and Dong Woo Cho. Critical Laboratory Evaluation of Asphalt Binders Modified by Refining Process. Proceedings of the Canadian Technical Asphalt Association, 49, 2004.

10. J. Haddock and Y. Tang. Investigation of the Performance of Neat and Modified Asphalt Binders. Joint Transportation Research Program Project No. C-36-56L, 2003.

11. Wise J. and R. Lorio. A Practical Guide for Estimating the Compaction Window Time for Thin-Layer Hot Mix Asphalt. Proceedings of the 8th Conference on Asphalt Pavements for Southern Africa (CAPSA'04) 12 – 16 September 2004. ISBN Number: 1-920-01718-6 Sun City, South Africa.

12. Mansell, T. Raveling in Hot-Mix Asphalt Pavements, http://www.graniterock.com/tnraveling.html.

13. Lodewikus ter Huerne, H. Compaction of Asphalt Road Pavements Using Finite Elements and Critical State Theory. CT&M Department, University of Twente, P.O. Box 217, 7500 AE, Enschede, the Netherlands.

14. Blankenship P., K. Mahboub and G. Huber. Rational Method for Laboratory Compaction of Hot Mix Asphalt. In *Transportation Research Record: Journal of the Transportation*

Research Board, No 1454, TRB, National Research Council, Washington, D.C., 1995, pp 144 – 15. State of Wisconsin Department of Transportation. Standard Specifications for Highway and Structure Construction, 1996.

16. Kitae Nam, Rodrigo Delgadillo and Hussain Bahia. Development of Guidelines for PG Binder Selection in Wisconsin, Report 0092-01-01. Wisconsin Highway Research Program. June 2005.

17. Delgadillo, R. and H.U Bahia. Rational Fatigue Limits For Asphalt Binders Derived From Pavement Analysis. *Journal of the Association of Asphalt Paving Technologists.* Vol. 74, 2005.

18. Bahia, H.U., M. Zeng and K. Nam. Considerations of Strain at Failure and Strength in Prediction of Pavement Thermal Cracking. *Journal of the Association of Asphalt Paving Technologists.* Vol. 69. Reno, Nevada. 2000.

19. Nam, K. Effect of Asphalt Modification on Failure Properties of Asphalt Binders. MSc Thesis, University of Wisconsin Madison, 2001.

20. Delgadillo, R., K. Nam & H. U. Bahia. Why do We Need to Change G*/sinδ and How? Road Materials and Pavement Design, Issue 1, 2006.

21. D'Angelo, J., R. Kluttz, R. Dongre, K. Stephens and L. Zanzotto. Revision of the Superpave High Temperature Binder Specification: The Multiple Stress Creep Recovery Test. *Journal of the Association of Asphalt Paving Technologists.* Vol. 76, 2007.

APPENDIX: DATABASE DESCRIPTION

A database was created as part of the research project. The program used was Microsoft Excel. The present section describes each of the Excel spreadsheets included in the file.

- General Information: Project ID (assigned by the WisDOT); location of the project and type of validation carried out (fatigue, rutting…). The project ID is the link between the information in different sheets.
- Materials: lab and field information for binder and mixture. Binder data includes compaction temperature, rutting parameters, fatigue parameters, and low temperature cracking parameters. Mixture data includes mixture type, nominal size of aggregate, and number of gyration. Some projects were sampled multiple times, so more than one value was obtained for some of the parameters.
- Pavement Structure: thickness and material type for each layer in the pavement structure. For some of the projects, there were more than one typical cross section.
- Traffic: ADT at the first year and final year; traffic distribution data; design ESALs and design speed.
- Weather: maximum and minimum temperatures for both, air and pavement.
- Section Information spread sheet: section ID, location of each section and direction of survey in each project. The sections are the specific locations where the projects were surveyed. The section ID is the same ID used in the WisDOT performance database.
- Performance: pavement's distress information including severity and extent. This surveys are carried out every other year, so it is the information available. The format used to

describe the severity and extent of distresses is the same described in the WisDOT PIF manual.